Project: “Monitoring Sea-water intrusion in coastal aquifers and Testing pilot projects for its mitigation” Interreg CBC Italy-Croatia 2014.-2020.

Priority Axis: Safety and resilience

Specific objective: Improve the climate change monitoring and planning of adaptation measures tackling specific effects, in the cooperation area

(D_3.4.4) Report on the groundwater and transport flow model application to the to the Croatian field site draft

Work Package 3: Studying

Activity 4: Numerical modelling

Partner in charge: PP4 (UNIST-FGAG)

Partners involved: PP4 (UNIST-FGAG), PP5 (CROATIAN WATERS), PP6 (DUNEA)

Final version

Public report

September, 2022

Contents

Introduction 3
Model description 4
Aquaveo GMS program 4
Numerical models 6
MODFLOW 6
MT3DMS 7
SEAWAT 8
Model build up – from input data to 3D grid 10
Input data 10
Borehole Module 10
TIN Module 16
3D Solid Module 17
3D Grid Module 19
Model solver packages setup 22
MODFLOW setup 22
MT3DMS setup 24
SEAWAT setup 27
Flow and transport boundary conditions 28
Flow boundary conditions 28
RIV Package 29
CHD Package 31
Specified Flow 34
EVT Package 35
RCH Package 35

Transport boundary conditions 37
Specified Concentration Boundary Conditions 37
Configuration of model steps 38
Definition of model steps 38
Spatial-temporal analysis of salinity fields 41
Calibration and model results 45
Flow steady state results 45
Transient flow results 46
Flow and transport steady state results 50
Transient flow and transport transient results 54
Calibration of results and definition of final model parameters 59
Results verification 63
Conclusion 72
Bibliography 73
List of figures 75

Introduction

The report has been done to give a comprehensive overview of modelled scenarios. The latter assumes an overview of input parameters used along the conducted model scenarios, mainly focused to local geological conditions found on site and meteorological and hydrological variables to be used for purpose of boundary and initial conditions setting up. Besides the input parameters and variable, report offers an overview of model background to enable clear insight and repetition of elaborated scenarios.

In its origin, the report is divided into two Results section, first one being focused to flow conditions and second one to dual density model results. This approach should serve as a logical way to take a reader into the problem, starting from site description, leading to implementation of local conditions into the model, giving the methodological overview, and latest, offering results in a straight way. Flow model results are supposed to offer information on local conditions, like irrigation system infrastructure, natural hydrological regime of Neretva and Mala Neretva, but also the sea level influence to piezometric state characterization of the site.

After flow conditions are obtained, dual density SWI model offers an insight to sea water caused concentration dynamics within the area of interest. The intention is to define the significance of relevant parameters to spatio-temporal characterization of concentration scalar field.

Model description

Aquaveo GMS program

The groundwater and transport flow model was made in Aquaveo GMS program. The Groundwater Modelling System (GMS) is a comprehensive graphical user environment for performing groundwater simulations. The entire GMS system consists of a graphical user interface (the GMS program) and a number of analysis codes (MODFLOW, MT3DMS, etc.).

GMS was designed as a comprehensive modelling environment. Several types of models are supported and facilities are provided to share information between different models and data types. Tools are provided for site characterization, model conceptualization, mesh and grid generation, geostatistics, and post-processing.
[1]

The interface for GMS is divided into twelve modules. A module is provided for each of the basic data types supported by GMS. As you switch from one module to another module, the Dynamic Tool Palette and the Menus change. This allows you to focus only on the tools and commands related to the data type you wish to use in the modelling process.

GMS modules are: TIN Module, Borehole Module, Solid Module, 2D Mesh Module, 2D Grid Module, 2D Scatter Point Module, 3D Mesh Module, 3D Grid Module, 3D Scatter Point Module, Map Module, GIS Module and UGrid Module.

Icon	Module
	TIN Module
	Borehole Module
	Solid Module
	2D Mesh Module
	2D Grid Module
	2D Scatter Point Module
	3D Mesh Module
	3D Grid Module
	3D Scatter Point Module
	Map Module
	GIS Module
	UGrid Module

Figure 1 GMS modules

Numerical models are programs that are separate from GMS that are used to run an analysis on a simulation. The simulation can be built in GMS, and then run through the numerical model program. GMS can then read in and display the results of the analysis. The following numerical models are currently supported in GMS: MODFLOE, MODPATH, MT3DMS, PEST, PHT3D, RT3D, SEAWAT, SEAM3D, MODEAM, UTEXAS, SEEP2D, FEMWATER and T-PROGS.

For this model MODFLOW, MT3DMS and SEAWAT were used.

Numerical models

MODFLOW

MODFLOW (originally called the Modular Three-Dimensional Finite-Difference GroundWater Flow Model) is a 3D, cell-centered, finite difference, saturated flow model developed by the United States Geological Survey [2]. MODFLOW can perform both steady state and transient analyses and has a wide variety of boundary conditions and input options. In GMS, MODFLOW can work with the 3D Grid module and 3D UGrid module.

Ground-Water Flow Equation

The partial-differential equation of ground-water flow used in MODFLOW is:

$$\frac{\partial}{\partial x}\left(K_{xx}\frac{\partial h}{\partial x}\right)+\frac{\partial}{\partial y}\left(K_{yy}\frac{\partial h}{\partial y}\right)+\frac{\partial}{\partial z}\left(K_{zz}\frac{\partial h}{\partial z}\right)+W=S_s\frac{\partial h}{\partial t} \quad (1)$$

where

K_{xx}, K_{yy}, K_{zz} – values of hydraulic conductivity along the x, y, and z coordinate axes, which are assumed to be parallel to the major axes of hydraulic conductivity [kg s^{-1}],
h – potentiometric head [m],
W – volumetric flux per unit volume representing sources and/or sinks of water, with W<0.0 for flow out of the ground-water system, and W>0.0 for flow in [s^{-1}],
SS – specific storage of the porous material [m^{-1}],
t – time [s].

Equation (1), when combined with boundary and initial conditions, describes transient three-dimensional ground-water flow in a heterogeneous and anisotropic medium, provided that the principal axes of hydraulic conductivity are aligned with the coordinate directions.

MT3DMS

MT3DMS (Modular Transport, 3-Dimensional, Multi-Species model) is a modular three-dimensional transport model for the simulation of advection, dispersion, and chemical reactions of dissolved constituents in groundwater systems [3]. MT3DMS uses a modular structure similar to the structure utilized by MODFLOW. MT3DMS is used in conjunction with MODFLOW in a twostep flow and transport simulation. Heads and cell-by-cell flux terms are computed by MODFLOW during the flow simulation and are written to a specially formatted HFF file.

The integrated MT3DMS transport (IMT) Process solves solute transport equation:

$$\left(1+\frac{\rho_b\, K_d^k}{\theta}\right)\frac{\partial(\theta C^k)}{\partial t} = \nabla\cdot(\theta \boldsymbol{D}\cdot\nabla C^k) - \nabla\cdot(\boldsymbol{q}C^k) - q'_s C_s^k \qquad (2)$$

where

ρ_b – bulk density (mass of the solids divided by the total volume) [kg m^{-3}],
K_d^k – distribution coefficient of species k [m^3 kg^{-1}],
C^k – concentration of species k [kg m^{-3}],
D – hydrodynamic dispersion coefficient tensor [m^2 s^{-1}],
q – specific discharge [m s^{-1}],
C_s^k – the source or sink concentration of species k [kg m^{-3}],

SEAWAT

SEAWAT is a three dimensional variable density groundwater flow and transport model developed by the USGS based on MODFLOW and MT3DMS [4]. SEAWAT v4 is based on MODFLOW 2000 and MT3DMS 5.2. SEAWAT includes two additional packages: VariableDensity Flow (VDF) and Viscosity (VSC).

GMS supports SEAWAT as a pre- and post-processor. The interface to SEAWAT relies on the interface to MODFLOW and MT3DMS. The input data for SEAWAT is generated by GMS and saved to a set of files including a MODFLOW model, an MT3D model if transport is used, and a SEAWAT model pointing to the MODFLOW and MT3D model's package files.

Three-dimensional computer program SEAWAT is used for simulation of saltwater intrusion, coupling MODFLOW for calculation of variable density, saturated groundwater flow (1), and MT3DMS solving solute transport equation (2).

The variable-density flow (VDF) Process solves the groundwater flow equation:

$$\nabla \cdot \left[\rho \frac{\mu_0}{\mu} \boldsymbol{K_0} \left(\nabla h_0 + \frac{\rho - \rho_0}{\rho_0} \nabla z \right) \right] = \rho S_{s,0} \frac{\partial h_0}{\partial t} + \theta \frac{\partial \rho}{\partial C} \frac{\partial C}{\partial t} - \rho_s q'_s \qquad (3)$$

where

ρ_0 – fluid density at the reference concentration and reference temperature [kg m^{-3}],

μ – dynamic viscosity [kg m^{-1} s^{-1}],

K_0 – hydraulic conductivity tensor of material saturated with the reference fluid [kg s^{-1}],

h_0 – hydraulic head measured in terms of the reference fluid of a specified concentration and temperature [m],

$S_{s,0}$ – specific storage, defined as the volume of water released from storage per unit volume per decline of h_0 [m^{-1}],

t – time [s],

θ – porosity [-],

C – salt concentration [kg m^{-3}],

q'_s – source or sink of fluid with density ρ_S [s^{-1}] .

$$\left(1+\frac{\rho_b K_d^k}{\theta}\right)\frac{\partial(\theta C^k)}{\partial t} = \nabla\cdot(\theta D\cdot\nabla C^k) - \nabla\cdot(qC^k) - q_s' C_s^k \quad (4)$$

where

ρ_b - bulk density (mass of the solids divided by the total volume) [kg m^{-3}],
K_d^k - distribution coefficient of species k [$m^3 kg^{-1}$],
C^k - concentration of species k [kg m^{-3}],
D - hydrodynamic dispersion coefficient tensor [m^2 s^{-1}],
q - specific discharge [m s^{-1}],
C_s^k - source or sink concentration [kg m^{-3}] of species k.

European Regional Development Fund

Model build up – from input data to 3D grid

Input data

Borehole Module and TIN Module (in combination with 2D Scatter Point Module) were used to transform data collected from the area of River Neretva Valley into form that is accepted by the model.

Borehole Module

The Borehole module of GMS can be used to visualize boreholes created from drilling logs or synthetic boreholes created manually and to construct three-dimensional cross sections between boreholes. These cross sections show the soil stratigraphy between two boreholes. Borehole data can be imported or created in GMS. Borehole data can be converted to other types of objects such as 2D scatter points, TINs, 3D meshes.
[5]

Boreholes were used as primarily input data for Aquaveo GMS. First in situ geological works in River Neretva Valley were performed in 1960s. In period from 1962 till 2019 more than 138 borehole logs were performed, but due to the limited technical capacities and constraints in the fulfilment of the full geological characterization, some older results are shown not to be reliable after comparison with upto-date results. Maximum depth of borehole logs is 125m and it is located in the middle of River Neretva Valley. Figure 2 shows spatial distribution of all boreholes in River Neretva Valley and area covered by the model. Only boreholes that are in inside of that area were used as input data for the model.

Figure 2 Spatial distribution of all boreholes in River Neretva Valley

Since borehole logs were made during the long period of time, soil classification differs from one borehole log to another. Logs made during 1960s and 1970s were made manually and soil classification was based on visual inspection. Borehole logs of more recant date have very specific soil classification based on measurements and results of tests performed on soil sample. Figure 3 shows borehole log from 1960s and Figure 4 shows borehole log of more recent date.

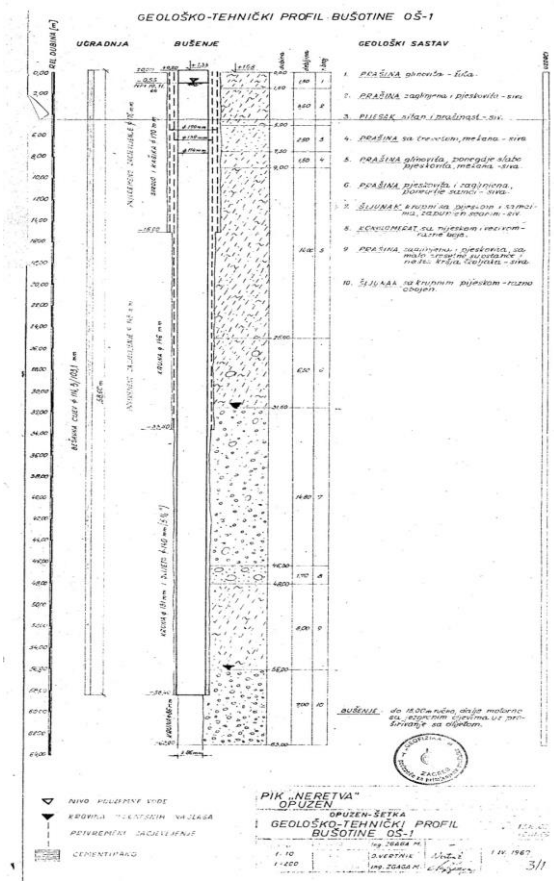

Figure 3 Borehole log from 1960s

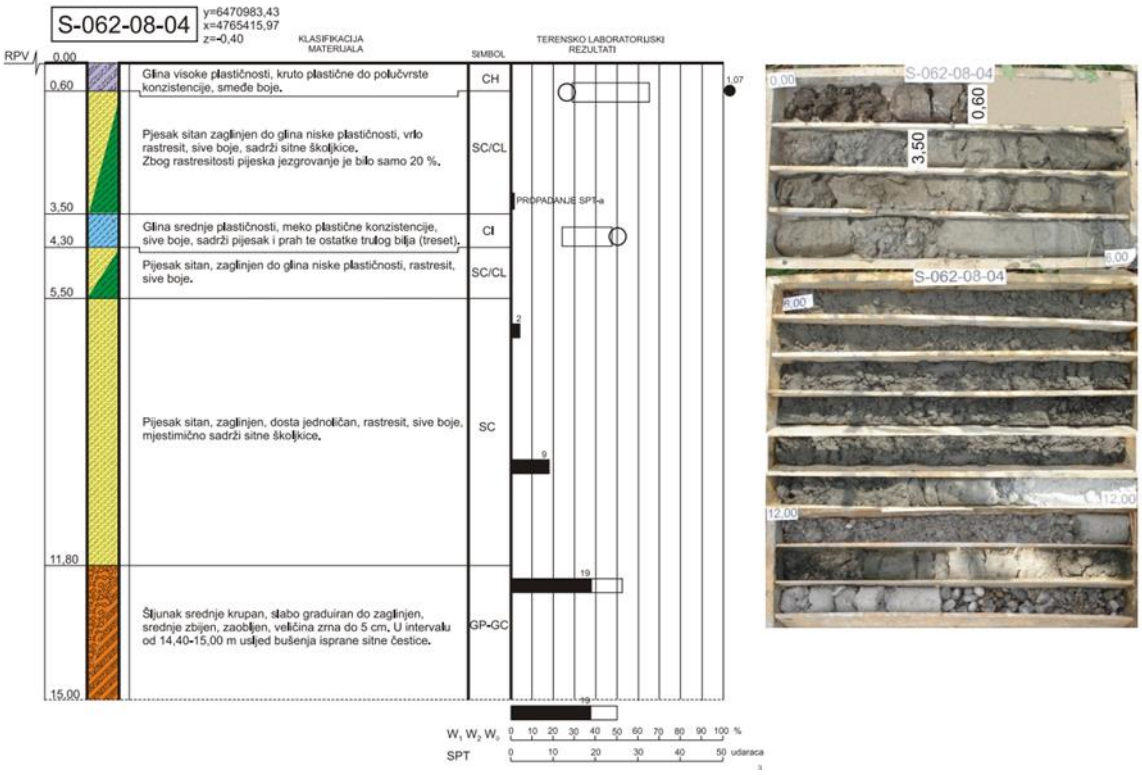

Figure 4 Borehole log from 2008

Geophysical investigations were performed at three locations at the mouth of Neretva River: the area around the Diga embankment, the area around Crepin channel, and in Krvavac settlement. Measurements were taken using the geoelectrical resistivity method. Resistivity measurements were performed by geoelectrical sounding (VES - Vertical electrical sounding) and 2D geoelectrical profiling, i.e. geoelectric tomography. The objective of investigations was to determine the geological structure of the terrain and depth down to the bedrock, and to assess the depth and surface distribution of saline deposits. A total of 8 geoelectric probes and 600 meters of tomography cross sections have been measured.

Maximum depth of additional investigation was 164 m and with this data, the position of bedrock in middle of River Neretva Valley was confirmed. All data collected by resistivity sounding was transformed in boreholes and by Borehole Module transferred in Aquaveo GMS.

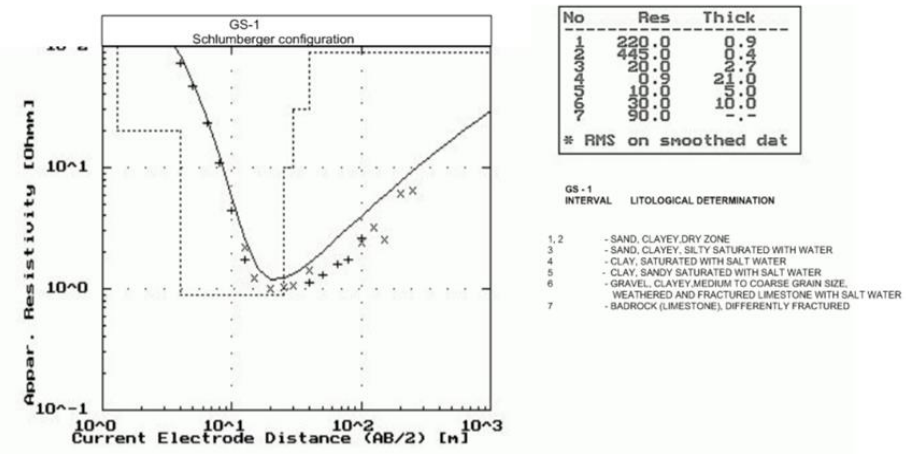

Figure 5 Resistivity sounding log

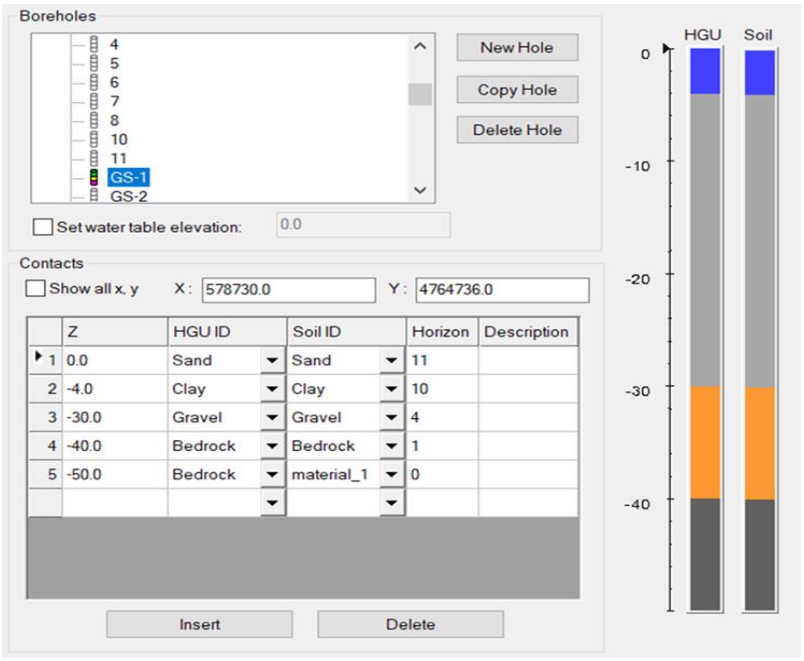

Figure 6 Resistivity sounding log transformed into borehole in GMS

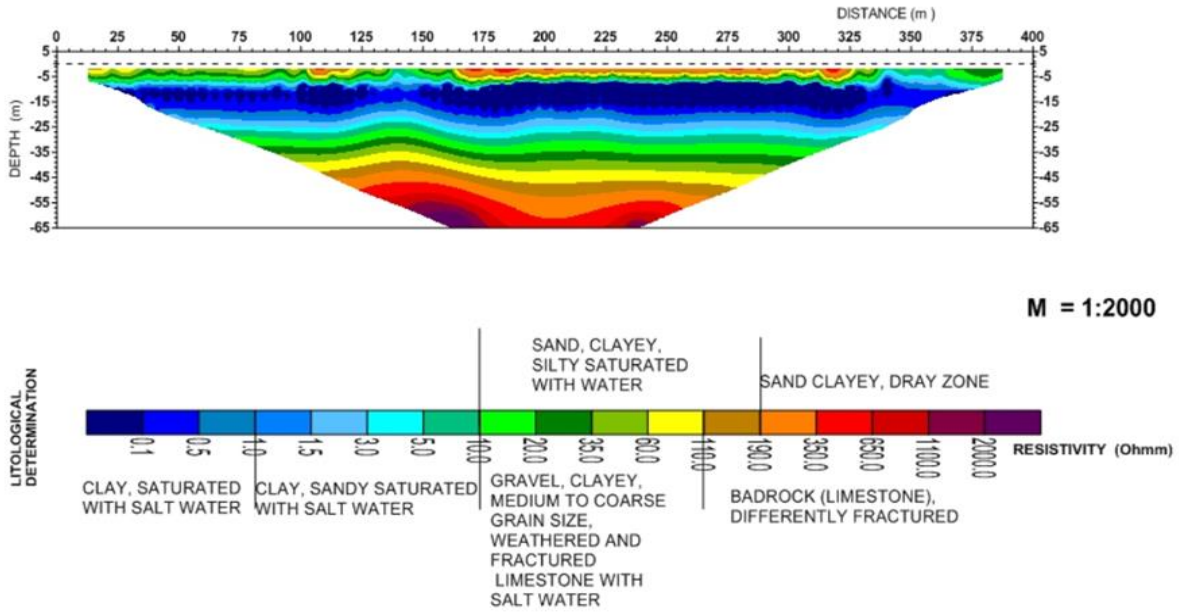

Figure 7 Geoelectric tomography log

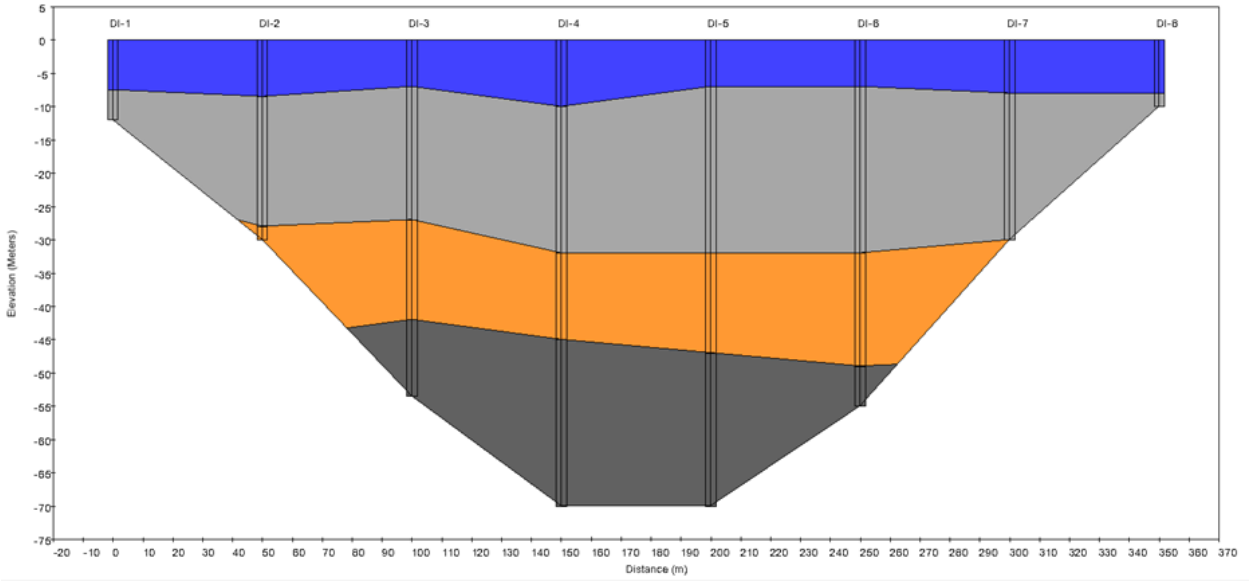

Figure 8 Geoelectric tomography log transformed in GMS cross-section

After adding all input data by Borehole module in Aquaveo GMS it was necessary to verify and select credible data. Since borehole logs were created during the long period of time, recent results were considered more reliable that those of older age. Also, if there was local disparity, the data was further verified and, in case of total deviation, removed.

Soil type classification was different from different type of input data and it was needed to specify representative soil types. Five soil types were chosen as representative soil types and their characteristics are defined based on borehole logs data and laboratory testing. Representative soil types are sand, clay, gravel A, conglomerate and gravel B. Figure 9 shows selected soil types and geological characteristics for specified parameters needed for the model. These geological characteristics were calibrated in later steps of model setup.

	ID	Name	Color/Pattern	Transparency (%)	Horizontal k (m/h)	Vertical k (m/h)	Horiz. anisotropy	Vert. anisotropy (Kh/Kv)	Specific storage (1/m)	Specific yield	Long. disp.	Porosity
All												
1	9	Sand		0.0	0.36	0.036	1.0	10.0	0.00004	0.25	10.0	0.3
2	2	Clay		0.0	0.000036	3.6e-006	1.0	10.0	0.0055	0.2	10.0	0.45
3	6	Gravel A		0.0	3.6	0.36	1.0	10.0	4.0e-006	0.0	10.0	0.35
4	4	Conglomerate		0.0	3.6e-008	3.6e-009	1.0	10.0	0.0055	0.0	10.0	0.45
5	3	Gravel B		0.0	3.6	0.36	1.0	10.0	4.0e-006	0.0	10.0	0.35
*												

Figure 9 Geological characteristics of representative soil types

TIN Module

TIN stands for Triangulated Irregular Network. TINs are used for surface modelling. TINs are formed by connecting a set of XYZ points with edges to form a network of triangles. They can be used to represent the surface of a geologic unit or the surface defined by a mathematical function.

TINs in GMS can be created manually, imported or created from other data objects. By default, GMS uses the Delaunay criterion to triangulate TINs. GMS provides a variety of tools and commands for manipulating TINs. TINs can be contoured, displayed in oblique view with mapped images and hidden surfaces removed, and have several other display options that can be set to visualize and understand the terrain surface better. GMS also contains custom settings for using TINs and allows TINs to be converted into other types of data, including solid models and 3D meshes. [5]

Detailed map of isohypses was obtained to determine spatial distribution of bedrock surface. Map of isohypses was transformed from 2D Scatter Point Module into TIN surface by using geostatistical interpolation. Bedrock was identified at the absolute depth of zero at the edge of valley area, to a maximum of 160 m below ground level found at the very central part of the valley, known as Crepina. Bedrock was used as bottom boundary condition for the whole area of River Neretva Valley and it is considered as no-flow boundary condition.

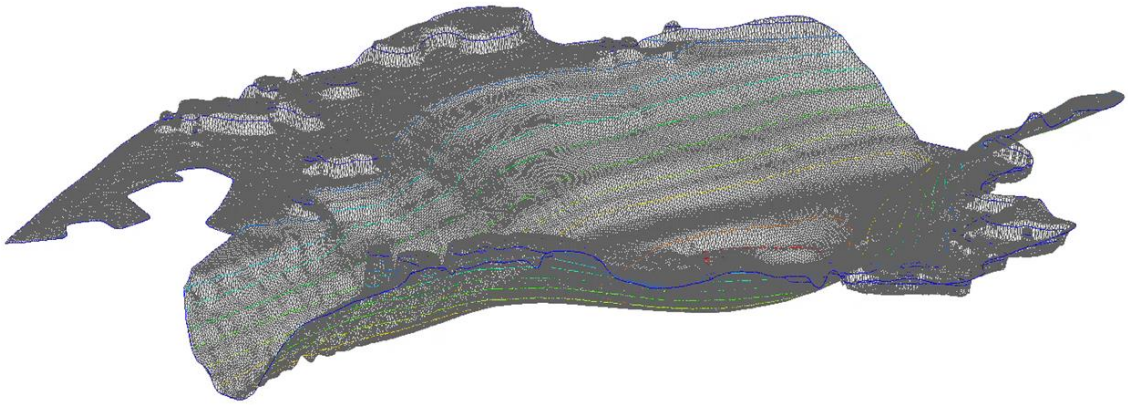

Figure 10 Bedrock surface in TIN Module

For defining upper surfaces of the model, geodesy of the whole area was used. Used geodesy data was very detailed and it contained definition of majority of channels and objects in River Neretva Valley area. Data was filtered and only river bed of River Neretva kept its geometric characteristics. For the rest of the Valley, the top elevations of channels were taken as upper surface of the model. All geodesy data was firstly transformed into 2D Scatter Points and after that in TIN surfaces.

3D Solid Module

The Solid module of GMS is used to construct three-dimensional models of stratigraphy using solids. Once such a model is created, cross sections can be cut anywhere on the model to create fence diagrams. Solids can be used to define layer elevation data for MODFLOW models or and to define a layered 3D mesh. [5]

3D solid model was created from borehole and TIN input data using command Horizons to Soils. For 3D soils all boreholes that passed verification were used. Conceptual model was used to define borders for the layer of conglomerate. Primary TIN was defined as outline of the whole model area. Top elevation TIN was defined based on upper surface geodesy and bottom elevation TIN was defined based on bedrock depth on the whole area. Inverse distance weighted interpolation method was used.

This 3D soils model is initial model for creation of 3D grid model. Solid model was made with total 5 solid types defined for boreholes. On the surface of the model there is sand with the average depth of 10 m. Below the sand there is a clay with the average depth of 20 m. Below clay, there are two layers of gravel and between them, on depth between 45-48 m, is the layer of conglomerate. The whole bottom surface of the model is bedrock. Figure 11 shows cross-section trough 3D solid model with TIN bedrock.

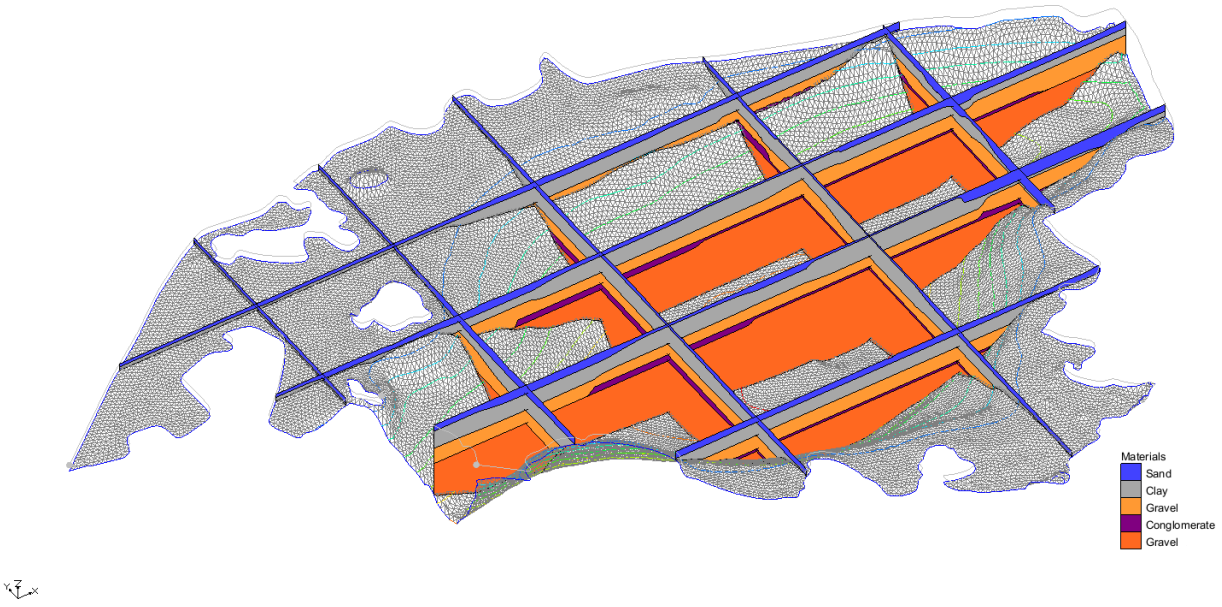

Figure 11 3D solid cross-sections

3D Grid Module

After creating and optimizing 3D solids it was possible to create 3D Grid that is base for MODFLOW model.

The 3D Grid module is used to create 3D Cartesian grids. These grids can be used for interpolation, isosurface rendering, cross sections, and finite difference modelling. Two types of 3D grids are supported in GMS: cell centred and mesh centred. When computations are performed on a mesh-centred grid, the computation points are the grid nodes or the corners of the grid cells. With a cell-centred grid, computations are performed at the cell centres.

When a dataset is imported to a cell-centred grid, there is one value in the dataset for each cell. To use contouring or fringing the values at the cell corners must be known. Therefore, whenever contouring or fringing is performed, the values at the cell centres are interpolated to the cell corners. Interpolation to cell corners is only done for visualization. All computations performed using the Data Calculator are performed on the original values at the cell centres. With mesh-centred grids, all visualization and computations are performed at the cell corners and no interpolation is necessary.

All of the model interfaces in the 3D Grid module are based on cell-centred grids. Mesh-centred grids are useful for interpolation and isosurface visualization since no extra interpolation is necessary.

Two approaches can be used to construct a MODFLOW simulation in GMS: grid or conceptual model. The grid approach works directly with the 3D grid and applies sources/sinks, and other model parameters on a cell-by-cell basis. Conceptual model approach works by converting conceptual model created in Map Data to 3D grid cells. [5]

For creation of this model, conceptual model approach for construction of 3D grid model was chosen. Outline of the model area was created as coverage in Map Module for initial conceptual model. Subsequently, all boundary conditions were created in Map Module coverages and transferred on 3D grid.

After the initial coverage was complete, it was possible to create the grid. The first step in creating the grid is to define the location and orientation of the grid using the grid frame. The grid frame represents the outline of the grid. It can be graphically positioned on top of the site map.

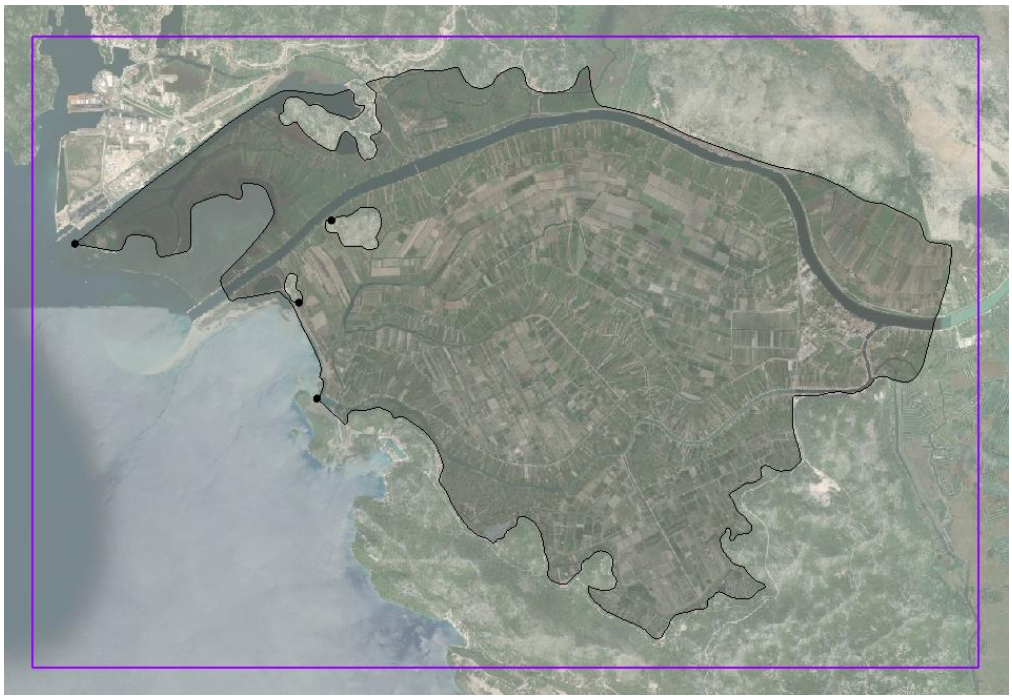

Figure 12 Conceptual model boundary and grid frame

With the coverages and the grid frame created, it was possible to create the grid. Map Module coverage with model outline was used do define boundaries for 3D grid. Option Feature Objects; Map to 3D Grid was used for 3D grid creation.

For our model we used grid without refinement with cell size of 50 m. Model soils were divided in 16 layers based on their thickness. 5 layers were used to represent sand, 2 layers for clay, 3 layers for upper gravel, 1 layers for conglomerate and 5 layers for bottom gravel.

After the grid is constructed, it was necessary to initialize the MODFLOW data before converting the conceptual model to a grid-based numerical model.

With the grid constructed and MODFLOW initialized, the next step was to define the active and inactive zones of the model. Each of the cells in the interior of any polygon in the local

sources/sinks coverage was designated as active, and each cell outside of all of the polygons was designated as inactive.

After creation of the 3D Grid and definition of active and inactive cells, Solids to MODFLOW command was used. The Solids to MODFLOW command brings up a dialog listing the three basic options associated with the Solids to MODFLOW command. Each option utilizes a different approach for converting the solid stratigraphy to the MODFLOW BCF input arrays. The three options are: Boundary Matching, Grid Overlay and Grid Overlay with Keq.

For our model we used Boundary Matching to connect Solids to MODFLOW layers. The goal of the boundary matching algorithm is to compute a set of elevation arrays that honour the boundaries between the stratigraphic units as closely as possible. Figure 11 shows 3D Grid with boundary matching option completed. After creation of 3D Grid model, it is possible to set all boundary and initial conditions for MODFLOW, MT3DMS and SEAWAT.

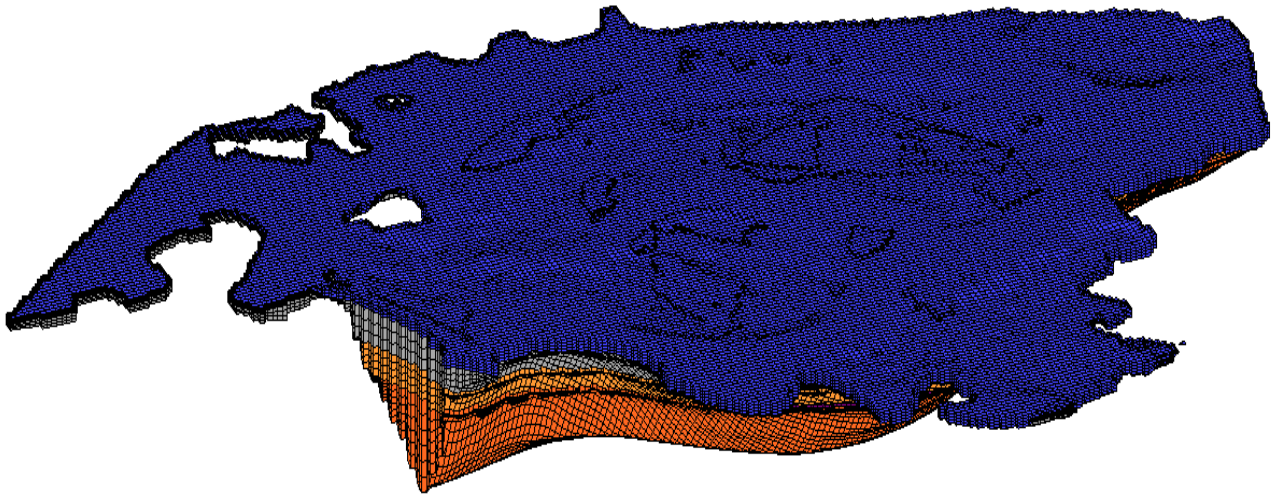

Figure 13 3D Grid model

Model solver packages setup

MODFLOW setup

MODFLOW is divided into a series of components called "packages." Each package performs a specific task. MODFLOW packages are divided in Flow packages, Solvers and Optional packages/processes.

Interfaces to four different flow packages are provided in GMS: the block-centred flow (BCF), the layer property flow (LPF), the hydrogeological unit flow (HUF), and the upstream weighting (UPW) packages.

For all our simulations layer property (LPF) flow package was used. For initial model simulation as layer property entry method material IDs were used and during calibration and verification date arrays as entry method was used. With the LPF package, it is needed to define the horizontal (K_h or HK) and vertical hydraulic conductivity (K_v or VK) for each layer. MODFLOW then computes the cell by cell conductance using conductivity values and the layer geometry. In LPF Package for every layer it is needed to define layer type (confined or convertible). All layers bellow clay are considered as confined. Cell wetting was not allowed. Initial material properties were defined as shown on Figure 9.

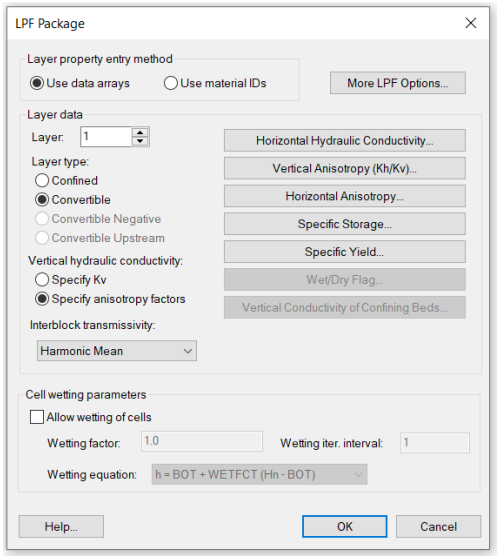

Figure 14 LPF Package dialog box

Solver packages provided in GMS are: Geometric Multi-Grid (GMG), Strongly Implicit Procedure (SIP1), Preconditioned Conjugate Gradient Method (PCG), Preconditioned Conjugate Gradient Solver with Improved Nonlinear Control (PCGN), Slice-Successive Overrelaxation Method (SOR1), Algebraic Multi-Grid for Systems Solver (SAMG or LMG), Direct Solver (DE4), Newton Solver (NWT) and Sparse Matrix Solver (SMS).

Abbrev.	Package Name	USGS	Description	Always Req'd?	Ext.
GMG	Geometric Multi-Grid	[9]	The Geometric Multigrid Solver is used to solve the finite difference equations in each step of a MODFLOW stress period.	Yes[2]	*.gmg
SIP1	Strongly Implicit Procedure	[10]	The Strongly Implicit Procedure package is used to solve the finite difference equations in each step of a MODFLOW stress period.	Yes[2]	*.sip
PCG	Preconditioned Conjugate Gradient Method	[11]	The Preconditioned Conjugate-Gradient package is used to solve the finite difference equations in each step of a MODFLOW stress period.	Yes[2]	*.pcg
PCGN	Preconditioned Conjugate Gradient Solver with Improved Nonlinear Control	[12]	The Preconditioned Conjugate-Gradient package is used to solve the finite difference equations in each step of a MODFLOW stress period.	Yes[2]	*.pcgn
SOR1	Slice-Successive Overrelaxation Method	[13]	The Slice-Successive Overrelaxation package is used to solve the finite difference equations in each step of a MODFLOW stress period.	Yes[2]	*.sor
SAMG or LMG	Algebraic Multi-Grid for Systems Solver	[14]	The LMG or Link-AMG package is used to solve the finite difference equations in each step of a MODFLOW stress period.	Yes[2]	*.lmg
DE4	Direct Solver	[15]	The DE4 package is used to solve the finite difference equations in each step of a MODFLOW stress period.	Yes[2]	*.de4
NWT	Newton Solver	[16]	The NWT package is used to solve the finite difference equations in each step of a MODFLOW-NWT stress period.	Yes[2]	*.nwt
SMS	Sparse Matrix Solver	[17]	The SMS package is used to solve the finite volume equations in each step of a MODFLOW-USG stress period.	Yes[2]	*.sms

Figure 15 List of solver packages provided for MODFLOW in GMS

The Geometric Multi-Grid (GMG) package is used to solve the finite difference equations in each step of a MODFLOW stress period.

With GMG package we are able to define inner convergence residual, maximum inner iterations, outer convergence residual, maximum outer iterations, damping parameter, damping options,

maximum damping, minimum damping, maximum head change, output flag, maximum head output, multi-grid preconditioner smoothing, multi-grid preconditioner coarsening and relocation parameter. Figure 16 shows GMG Package settings for our model.

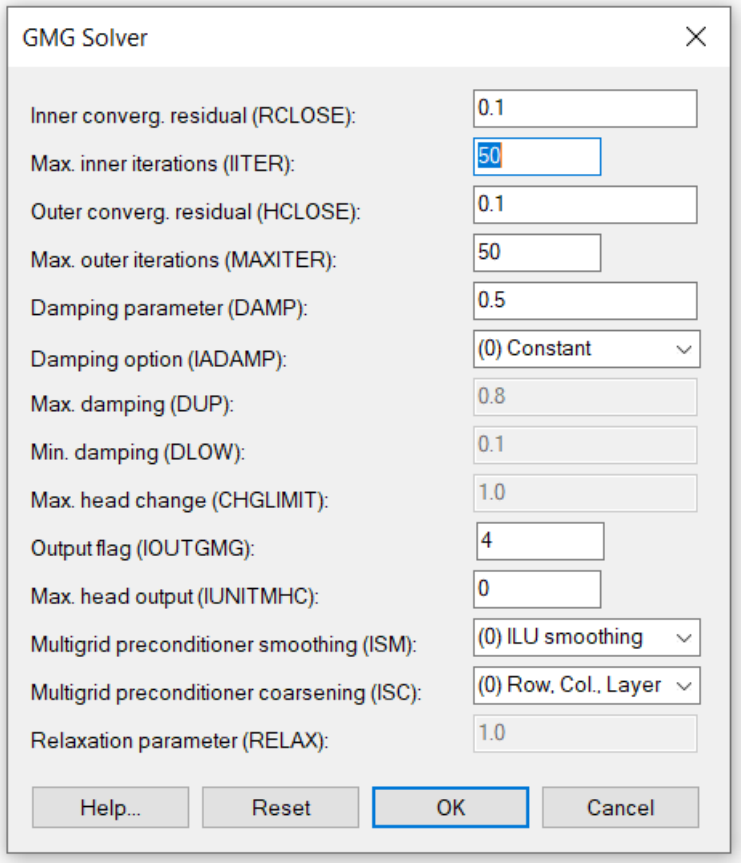

Figure 16 GMG Solver settings

MT3DMS setup

MT3DMS is divided into a series of packages and each of them performs a specific task. Some of the packages are always required for a simulation, and some are optional. The MT3DMS packages supported in the GMS interface are listed in the following table:

Package Name	Abbrev.	Decription	Always Req'd?
Basic Transport Package	BTN	Handles basic tasks that are required by the entire transport model. Among these tasks are definition of the problem, specification of the boundary and initial conditions, determination of the step size, preparation of mass balance information, and printout of the simulation results.	YES
Advection	ADV	Solves the concentration change due to advection with one of the three mixed Eulerian-Langrangian schemes included in the package: MOC, MMOC, or HMOC	NO
Dispersion	DSP	Solves the concentration change due to dispersion with the explicit finite difference method.	NO
Sink & Source Mixing	SSM	Solves the concentration change due to fluid sink/source mixing with the explicit finite difference method. Sink/source terms may include wells, drains, rivers, recharge, and evapotranspiration. The constant-head boundary and general-head-dependent boundary are also handled as sink/source terms in the transport model.	NO
Chemical Reactions	RCT	Solves the concentration change due to chemical reactions. Currently, the chemical reactions include linear or nonlinear sorption isotherms and first-order irreversible rate reactions (radioactive decay or biodegradation).	NO
Generalized Conjugate Gradient Solver	GCG	This package can be used to implicitly solve the dispersion, source/sink, and reaction terms of the transport equation.	NO
Transport Observation	TOB	Outputs concentration at observation points and mass fluxes at groups of source/sink boundary conditions.	NO
PHT3D-PHREEQC Interface	PHC	Used by PHT3D to define options for species related to PHREEQC geochemical reactions.	NO

Figure 17 List of MT3DMS packages provided in GMS

The information defined in the Basic Transport Package includes the computational time intervals (stress periods), an array defining which cells are inactive and which cells have constant concentration, an array defining aquifer porosity, and array of starting concentration values. The input data for the Basic Transport Package must be entered before editing any of the other packages in the MT3DMS simulation.

Basic Transport Package is used to specify which of the packages are to be used in the simulation. There are Advection package, Dispersion Package, Source/sink mixing package, Transport observation package and Chemical reaction package available to use with MT3DMS. MT3DMS is a multi-species transport model. It can track the migration and concentration of several species at once. So, it is needed to define the number of species in the simulation and the name and type of each species.

For out model we used advection package, dispersion package and source/sink mixing package. In advection package Standard finite difference method was used as solution scheme. In dispersion package ratio of horizontal and vertical transverse dispersivity to longitudinal dispersivity is defined as 0.1 and effective molecular diffusion coefficient is defined as 10E-9.

The Generalized Conjugate Gradient (GCG) Solver is used to solve the dispersion, source/sink, and reaction terms of the transport equation.

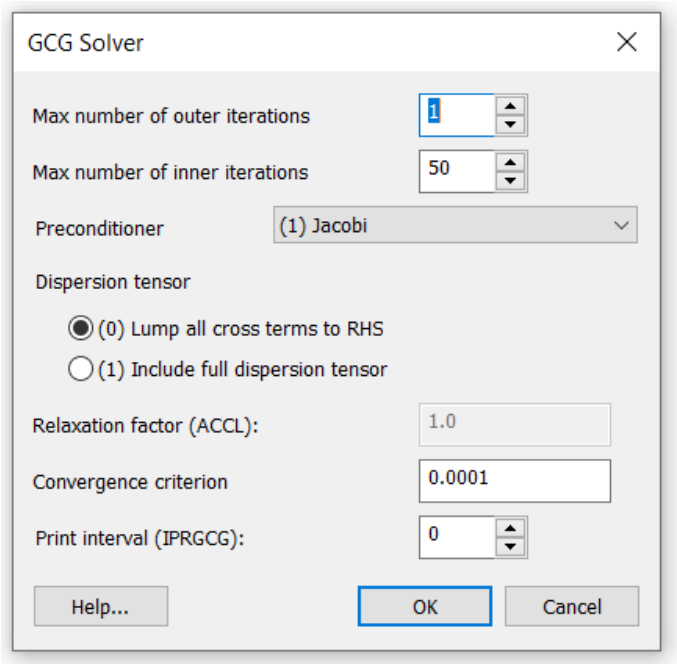

Figure 18 GCG solver setup

SEAWAT setup

SEAWAT specific packages include the Variable-Density Flow (VDF) and Viscosity (VSC) packages. The package dialogs for both packages are available under the SEAWAT menu. For the package menu items to be available, the packages must first be enabled from the SEAWAT Global Options dialog.

For our model we used VDF package. The VDF package can be used in a SEAWAT simulation to model the effects of concentration on fluid density. Figure 19 shows all input values used for our model.

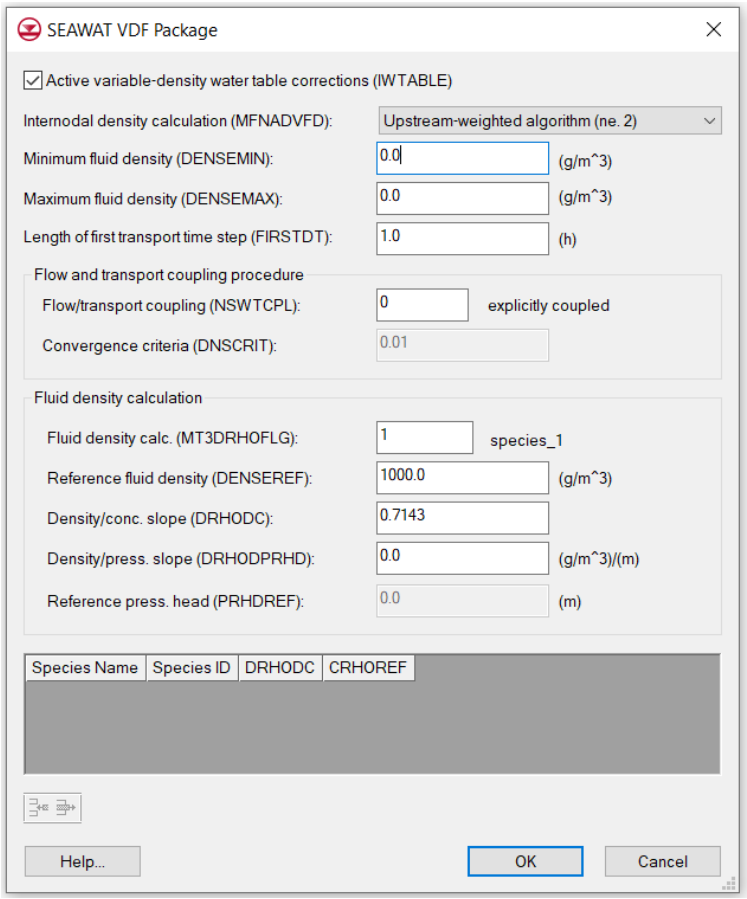

Figure 19 SEAWAT VDF Package

Flow and transport boundary conditions

Flow boundary conditions

After defining 3D Grid and initiating MODFLOW, it was needed to define boundary conditions for every element defined in conceptual model. Optional packages perform a specific task and were used to simulate boundary conditions. The boundary condition of the model is no-flow boundary except it is not defined otherwise.

Abbrev.	Package Name	USGS	Description	Always Req'd?	Ext.
BFH	Boundary Flow and Head Package	[18]	Used with MODFLOW-LGR to use coupled flows and heads when running parent or child model independently.	No	*.bfh_hed, *.bfh_flw
CLN	CLN Process		MODFLOW-USG process to simulate Connected Linear Network.	No	*.cln
DRN1	Drain Package	[19]	Simulates drain type boundary conditions.	No	*.drn
DRT1	Drain Return Package	[20]	Simulates drain return type boundary conditions.	No	*.drt
EVT1	Evapotranspiration Package	[21]	Simulates the effect of evapotranspiration in the vadose zone.	No	*.evt
ETS1	Evapotranspiration Segments Package	[22]	"allows simulation of evapotranspiration with a user-defined relation between evapotranspiration rate and hydraulic head."	No	*.ets
GAGE	Gage Package	[23]	Allows SFR and lake gaging stations. Gaging station prints time series values for gage location.	No	*.gag
GHB1	General Head Boundary Package	[24]	Simulates a general purpose head-dependent source/sink. Commonly used to simulate lakes.	No	*.ghb
GNC	Ghost Node Correction Package		Only in MODFLOW-USG, corrects for cells whose connector does not perpendicularly bisect the face.	No	*.gnc
HFB1	Horizontal Flow Barrier Package	[25]	Simulates the effect of horizontal flow barriers such as sheet piles and slurry trenches.	No	*.hfb
LAK3	Lake Package	[26]	A more sophisticated alternative to the typical approach of using the General head package to simulate the effect of lakes and reservoirs. Computes the stage based on the water budget unlike the GHB.	No	*.lak
MNW1	Multi-Node Well 1 Package	[27]	older revision of MNW package used to simulate wells that extend over more than one cell.	No	*.mnw
MNW2	Multi-Node Well 2 Package	[28]	updated revision of MNW1 package used to simulate wells that extend over more than one cell.	No	*.mnw2
RCH1	Recharge Package	[29]	Simulates recharge to the groundwater from precipitation.	No	*.rch
RIV1	River Package	[30]	Simulates river type boundary conditions.	No	*.riv
SFR2	Streamflow-Routing Package	[31]	Simulates the exchange of water between the aquifer and surficial streams. Includes routing and automatic computation of stage. Parameters for sensitivity analysis or parameter estimation are NOT supported.	No	*.sfr
STR1	Stream-Routing Package	[32]	Simulates the exchange of water between the aquifer and surficial streams. Includes routing and automatic computation of stage. Parameters for sensitivity analysis or parameter estimation are NOT supported.	No	*.str
CHD1	Time Variant Specified Head Package	[33]	Simulates specified head boundary conditions where the head is allowed to vary with time.	No	*.chd
SUB1	Subsidence Package	[34]	Simulates simulates aquifer compaction and land subsidence.	No	*.sub
SWI2	Seawater Intrusion Package	[35]	Simulates variable-density seawater intrusion in MODFLOW-2005.	No	*.swi
WEL1	Well Package	[36]	Simulates injection/extraction wells.	No	*.wel
UZF1	Unsaturated-Zone Flow Package	[37]	Simulate percolation of water through the unsaturated zone.	No	*.uzf

Figure 20 GMS optional packages

RIV Package

RIV Package is used to simulate rivers and channels in GMS. When the river attribute is assigned to an arc, the conductance is applied uniformly over the arc, but separate elevations and stage values are applied to each of the nodes on the ends of the arc. The elevation and stage are assumed to vary linearly between the nodes. When a river object is defined using a polygon or a point, all of the values are assigned directly to the cell(s) overlapped by the polygon or point. [5]

In our model we have simulated both rivers and drains with RIV package. For each river head stage and bottom elevation was defined based on geodesy and in situ measurements.

Tide gauge measurements and limnigraph measurements were taken as head boundary condition for River Neretva. To define Mala Neretva head values of “Opuzen mouth downstream” (Opuzen ušće nizvodno OUN) and “floodgate mouth upstream” (ustava ušće uzvodno UUU) were used as boundary conditions. For channels south from River Neretva head values of pumping station Modrič and head values of channel Jasenska were used as boundary condition. For channels south from Mala Neretva head values of pumping station Prag-Vidrice and head values from Mala Neretva were used to determine head values for the channels. Values were linear distributed between channels.

Bottom elevation for river Neretva, Mala Neretva and channels was determined based on geodesy of the area.

River (RIV) boundary condition type includes a conductance parameter. MODFLOW uses the conductance to determine the amount of water that flows in or out of the model due to the boundary condition stresses. For our model constant value of conductance was used. It was determent within the process of calibration.

Figure 21 Boundary conditions defined with RIV package

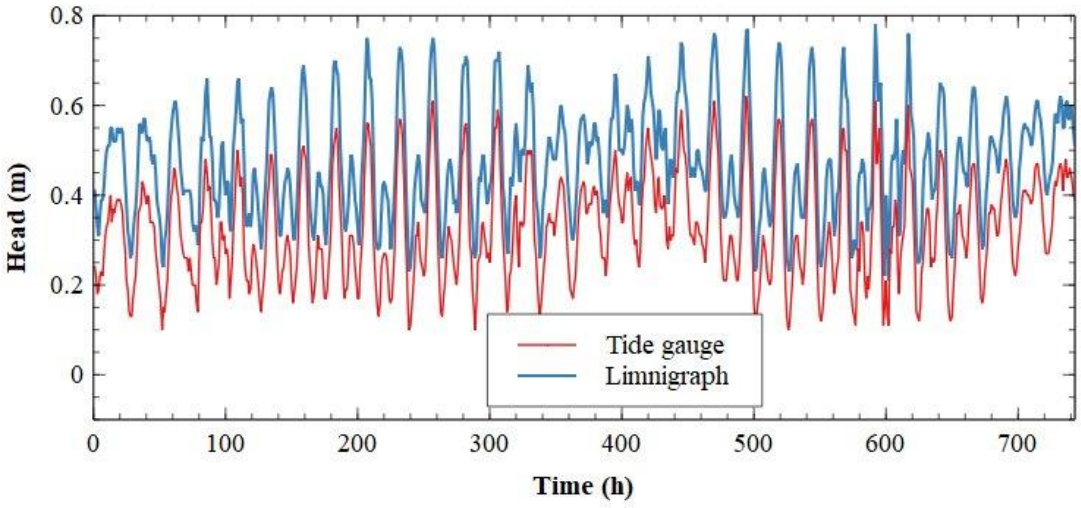

Figure 22 Tide gauge and limnigraph values for July 2021

CHD Package

The Constant Head Designation (CHD) is time variant specified head that reads data every stress period, which makes changing the head at constant-head cells throughout a simulation possible.

When the specified head attribute is assigned to a polygon, the head is assigned uniformly over the entire polygon. When assigned to an arc, separate head values are applied to each of the nodes on the ends of the arc and the head is assumed to vary linearly between the nodes. When the attribute is assigned to a point, the head is assigned directly to the cell containing the point. [5]

In the model CHD package is used to simulate seawater boundary condition and boundary condition for pumping stations Modrič and Prag-Vidrice. For pumping stations Modrič and Prag-Vidrice head values from field measurements were used.

Sea boundary condition was divided and separately defined for confined and unconfined aquifer. Tide gauge measurements were taken as time variant head boundary condition for seawater for unconfined aquifer (layers 1-5).

Confined aquifer – piezometric head boundary condition

Based on the assumption that unconfined aquifer starts at coastline with vertical face, the semipermeable layer and confined aquifer extend under the sea for distance L with an outlet-capping, beneath confined aquifer is impermeable layer and all the layers extend landward infinitely. All three aquifer units are assumed to be homogenous and with constant thickness. The flow is assumed to be one-dimensional (horizontal) in confined aquifer and vertical in semipermeable layer [6], [7]. The water table fluctuations are neglected in unconfined aquifer due to the difference between specific yield in unconfined aquifer and storativity in confined aquifer [8]. Specific yield is usually several orders of magnitude larger than storativity and can dump water table fluctuations more effectively [8]. Furthermore the density between groundwater and seawater is neglected as well ([6], [7], [9].

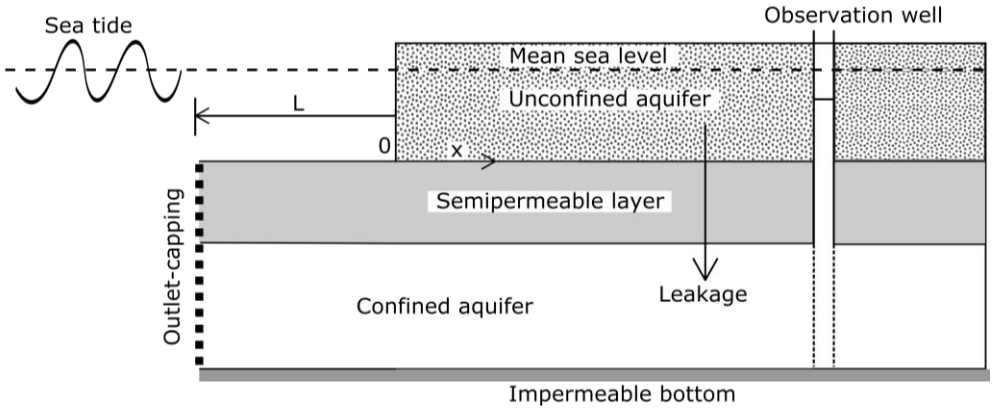

Figure 23 Conceptual model of the Neretva Valley aquifer

Based on the assumptions above mentioned and shown in Figure 23 and the theory of leaky, elastic aquifers the mathematical model of flow in confined aquifer can be written as [8], [10]:

1. In offshore confined aquifer

$$S\frac{\partial h}{\partial t} = T\frac{\partial^2 h}{\partial x^2} + SL_e\frac{\partial h_s}{\partial t} + L_s(h_s - h), \quad -L < x < 0 \quad (1)$$

2. In inland confined aquifer

$$S\frac{\partial h}{\partial t} = T\frac{\partial^2 h}{\partial x^2} + L_s h, \quad x \geq 0 \quad (2)$$

Where h(x,t) is hydraulic head [L], S and T are storativity and [-] and transmissivity [L^2T^{-1}] of the confined aquifer. Ls is specific leakage [T^{-1}] of the semipermeable layer, hs is the sea level at time t and Le represents the loading efficiency [-].

Loading efficiency represents the percentage of pressure that is transferred from sea level variations through semipermeable layer in offshore [8], [10].

Due to the fact that conventional numerical models (e.g. SEAWAT, COMSOL, SUTRA) cannot incorporate the effect of the Loading efficiency in the numerical simulations [11] the boundary condition used in the numerical model in the confined aquifer is calculated using the equations 1 and 2.

Using the equation 1 and 2 for the offshore and inland flow in confined aquifer the 1D finite difference model with Euler's explicit method is developed in Python environment with capacity of calculating the h(0,t).

Sea level fluctuations are taken from existing monitoring network in the Neretva Valley for the duration from 1st July 2022 – 15th October 2022 as offshore boundary condition, while the groundwater level of the same length is taken from D1 piezometer for inland boundary condition. The unknown parameters L, Le, Ss, k are taken from the research conducted by [12]. Respectively: L=1400 [m], Le=0.77 [-], Ss = 3e-6 [1/m], k=23 [m/h]. The amount of leakage through the semipermeable layer can be neglected [12].

The result and the time series that will be used in the numerical model as a seaward boundary condition in confined aquifer can be seen in Figure 2.

Figure 24 CHD boundary conditions for seawater and pumping stations

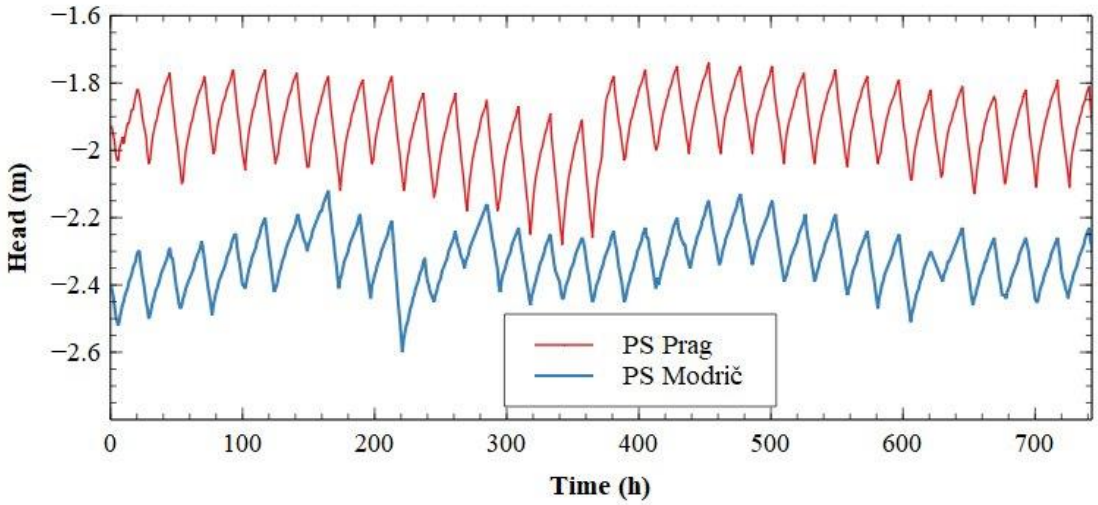

Figure 25 PS Prag and PS Modrič values for July 2021

Specified Flow

For Opuzen boundary condition Specified Flow package was used. Specified flow boundary condition distributes flow values along the arch. It is possible to set constant and time variant flow rate. In the model Specified Flow was used to describe flow in confined layers of gravel. It was determent within the process of calibration. [5]

Figure 26 Specified flow in the layer of gravel

EVT Package

The Evapotranspiration package is used to simulate the effect of plant transpiration and direct evaporation by removing water from cells during a simulation. Evapotranspiration (ET) is typically defined by specifying values for each stress period for each vertical column in the grid. The values consist of an elevation, an ET extinction depth, and a maximum ET rate. The elevation is an absolute elevation and the ET extinction depth (measured positive downward) is relative to the specified elevation. If the water table rises above the specified elevation, the evapotranspiration occurs at the maximum ET rate. If the water table falls below the ET extinction depth, evapotranspiration ceases. If the water table elevation lies between these two extremes, the evapotranspiration rate varies linearly with depth. [5]

RCH Package

The Recharge package is used to simulate recharge to an aquifer due to rainfall and infiltration. Recharge is typically defined by specifying a recharge value for each stress period for each vertical column in the grid. The recharge value represents the amount of water that goes into the groundwater system and not the amount of precipitation. The units of recharge are length/time. [5]

Recharge package was used only in transient simulations.

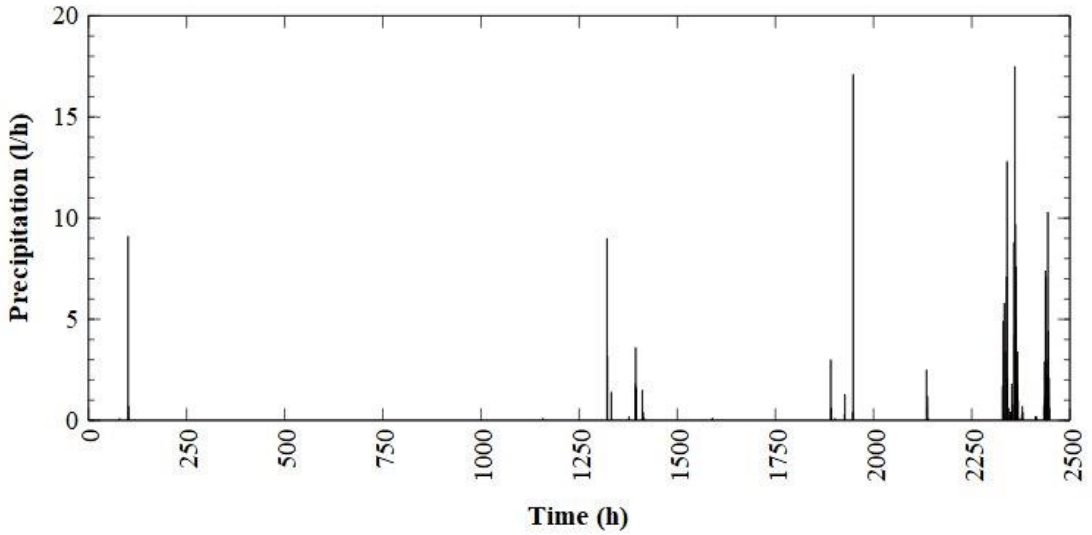

Figure 27 Precipitation in period July-September 2021

Transport boundary conditions

Specified Concentration Boundary Conditions

Specified concentration was the only transport boundary condition used. With specified concentration boundary conditions, a concentration value is assigned to the arc. This boundary condition was used when defining sea water concentration boundary condition, River Neretva concentration boundary condition for specified scenarios and concentration boundary condition for specific channels.

Along the sea line specific concentration was defined with constant value of 36 g/L. For River Neretva specific concentration was defined to simulate salt water wedge during the summer period and it was used only for specified scenarios. The value of the concentration was set on 36 g/l.

In transient simulation specified concentration was determined for specific channels. The value of concentration was determined based on field measurements.

Figure 28 Specified concentration boundary condition

Configuration of model steps

Definition of model steps

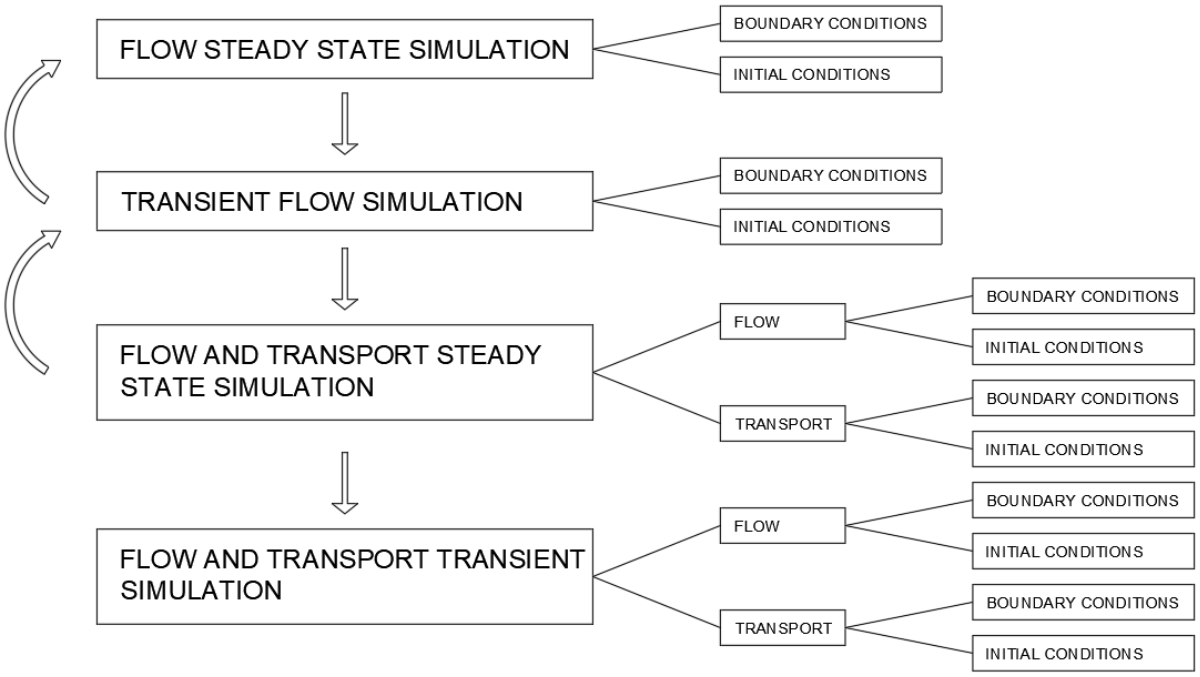

Figure 29 Model steps

To set up the model correctly it is important to understand the steps for model setup that are shown on Figure 29.

After setting geometry of the model, defining all boundary conditions in conceptual model and defining all solvers, first step is to obtain flow steady state simulation. Settings for flow steady state simulation are given as model type in MODFLOW Global/Basic Package.

Boundary conditions for flow steady state simulation were mean values of determined boundary condition values. Initial condition for flow steady state simulation is given in MODFLOW Global/Basic Package as option “Starting heads equal grid top elevation”. MODFLOW Global/Basic Package with all options for steady state is shown on Figure 30.

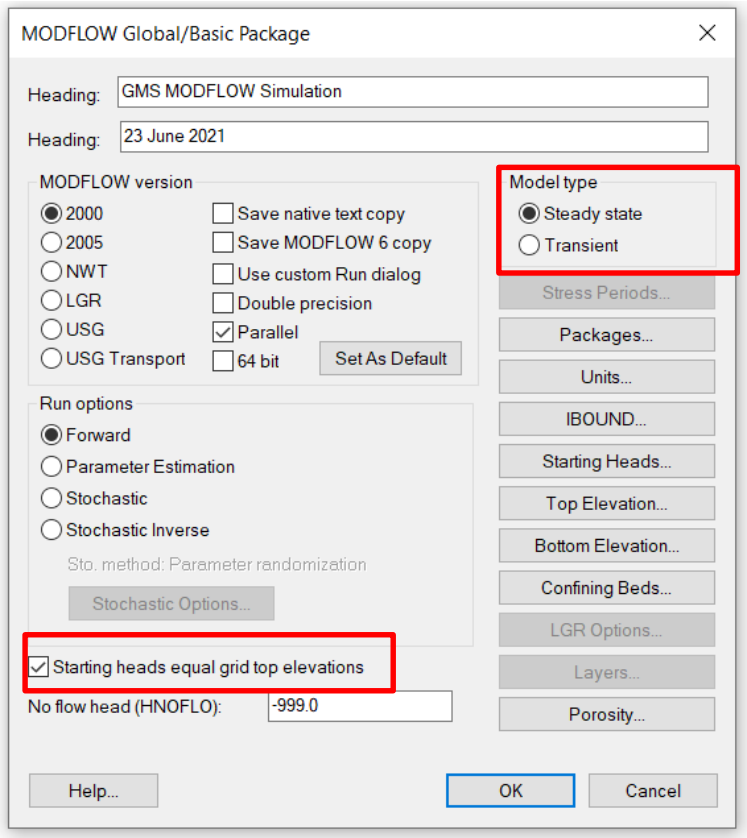

Figure 30 MODFLOW Global/Basic Package settings for flow steady state simulation

Second step of model setup was to obtain transient flow simulation. Boundary conditions for transient flow simulations were time variant values of determined boundary condition. For transient simulation it is needed to choose transient model type in MODFLOW Global/Basic Package and set number of stress periods in Stress Period menu. Transient flow simulation for our model is set for one month or 744 hours in model units. Initial condition for transient flow simulation were head results of flow steady state simulation.

Third step of model setup was to obtain flow and transport steady state simulation. This simulation was set as transient simulation in MODFLOW Global/Basic Package with 500 stress periods (each stress period presents one year). Flow and transport steady state simulation set as transient model was acceptable as steady state if there were no changes in head or concentration values during the time.

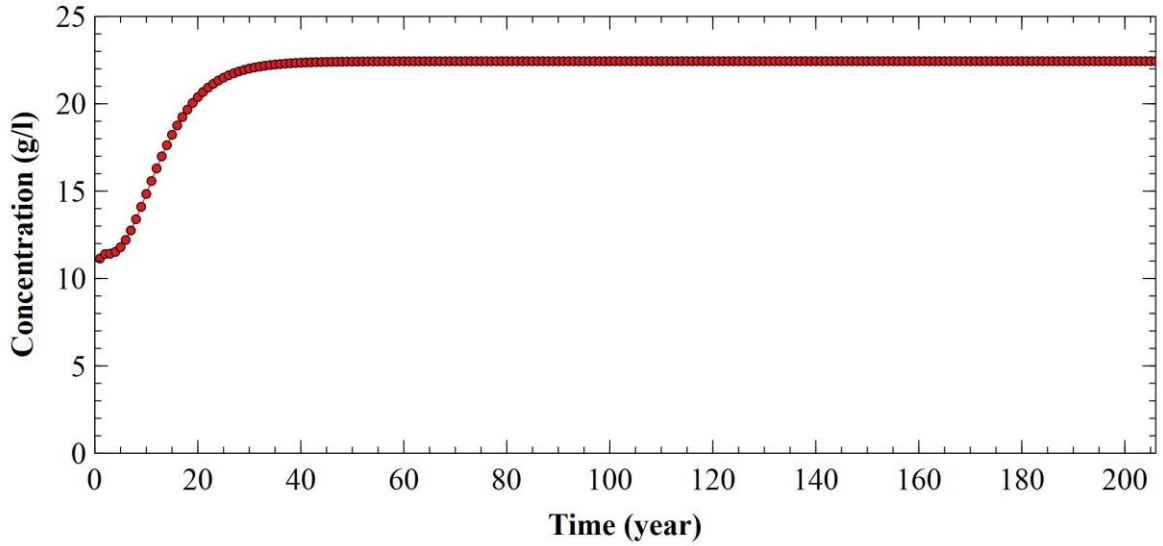

Figure 31 Concentration in one cell during the time and achievement of the steady state

Flow boundary conditions for coupled steady state simulation were mean values of determined boundary condition values. All values were set as constant transient values for 500 stress periods. Flow initial condition for coupled steady state simulation were head results of flow steady state simulation.

Transport boundary conditions for coupled steady state simulation was concentration value of 36 g/l along the sea line and in River Neretva. Boundary conditions for Opuzen, Mala Neretva and channels were defined as $dC/cX \neq 0$, $dC/dZ \neq 0$. Transport initial condition for coupled steady state simulation was concentration value of 0 g/l for the whole area of the model.

Last step of model setup was to obtain transient flow and transport simulation. Flow boundary conditions for transient flow and transport simulations were time variant values of determined boundary condition. Values of all boundary conditions were set for 744 hours. Flow initial condition for transient flow and transport simulation were head results of flow steady state simulation.

Transport boundary conditions for transient flow and transport simulation was the value of 36 g/l along the sea line and in River Neretva. Concentration boundary condition was set for channel

Jasenska and Vidrice since concentration measurements were available for those locations. Boundary conditions for Opuzen, Mala Neretva and the rest of the channels were defined as $dC/cX \neq 0$, $dC/dZ \neq 0$. Transport initial condition for transient flow and transport simulation were the values of concentration obtained in flow and transport steady state simulation.

Spatial-temporal analysis of salinity fields

To gain insight into change in salinity fields caused by different transport boundary condition for River Neretva, two different flow and transport steady state simulation were obtained. Those two simulations present scenarios for winter and summer period. Aim of these scenarios was to demonstrate main directions of entry and spread of saltwater in River Neretva Valley. Transport boundary conditions for the sea was the value of 36 g/l and $dC/cX \neq 0$, $dC/dZ \neq 0$ for Opuzen, Mala Neretva and channels.

Boundary conditions for River Neretva were:

a) Winter period – River Neretva concentration 0 g/l in all layers
b) Summer period – River Neretva concentration 36 g/l in all layers

Steady state models were gained for this two scenarios. For every scenario it took between 200 and 500 years for the model to gain steady state. Steady state values were confirmed when there were no changes in head or concentration values during the time. For all simulations horizontal hydraulic conductivity for the layer of clay was set on 0.0005 m/s while the geological characteristics for the rest of the soils were as in Figure 9. Increase in horizontal hydraulic conductivity for the layer of clay was necessary for steady state achievement and it increases salt water intrusion giving the model results with increased values of concentration.

Figure 32, Figure 33 and Figure 34 show transport steady state results for winter period. The only source of salt water intrusion is a sea with concentration of 36 g/l. Impact of channel Jasenska and Mala Neretva in mitigation of salt water intrusion is noticed in surface layer.

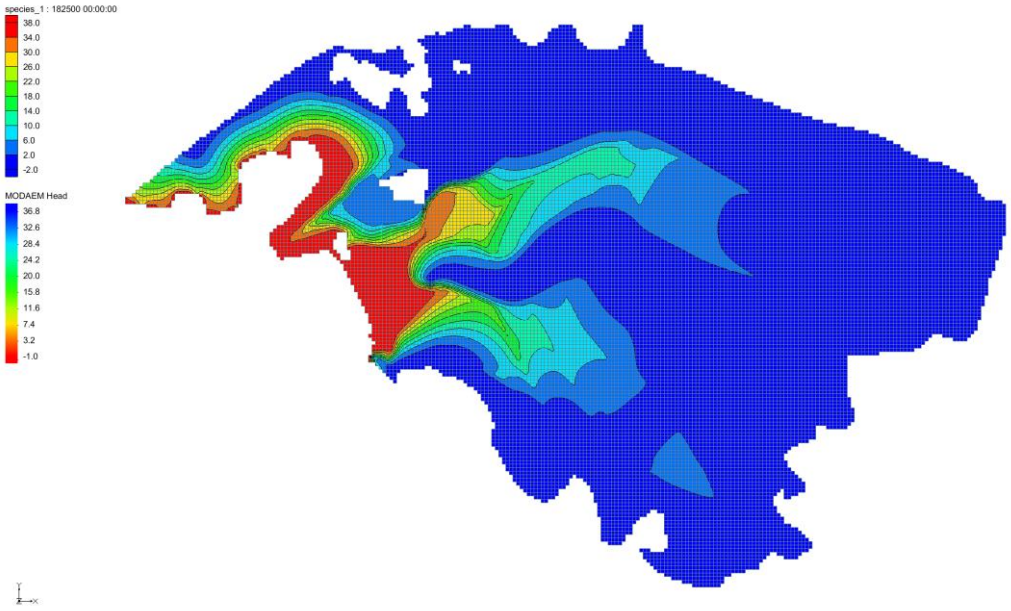

Figure 32 Salinity field for winter period in surface layer

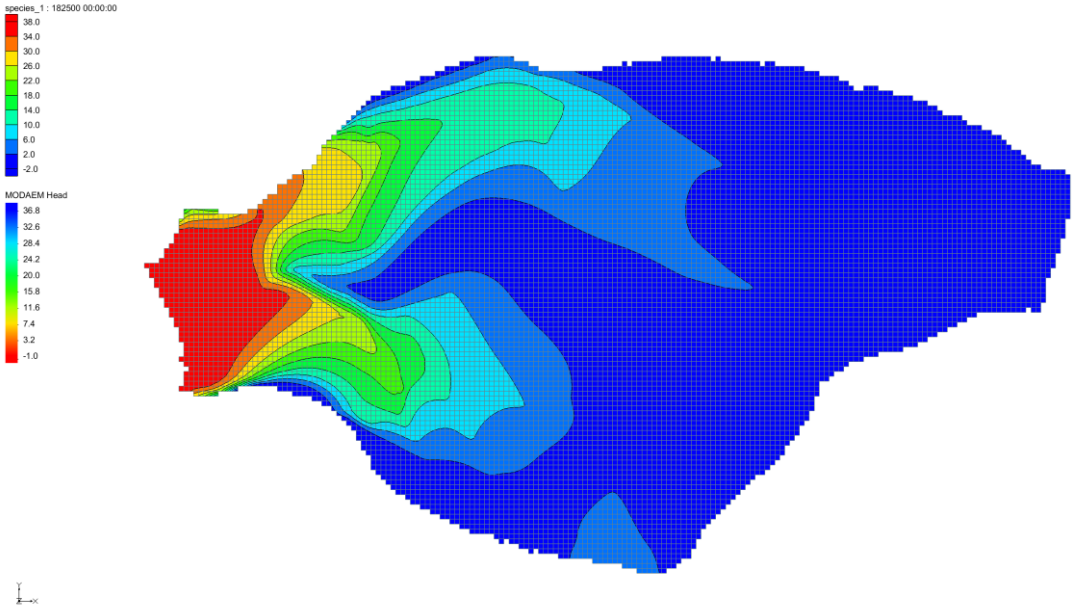

Figure 33 Salinity field for winter period in gravel layer

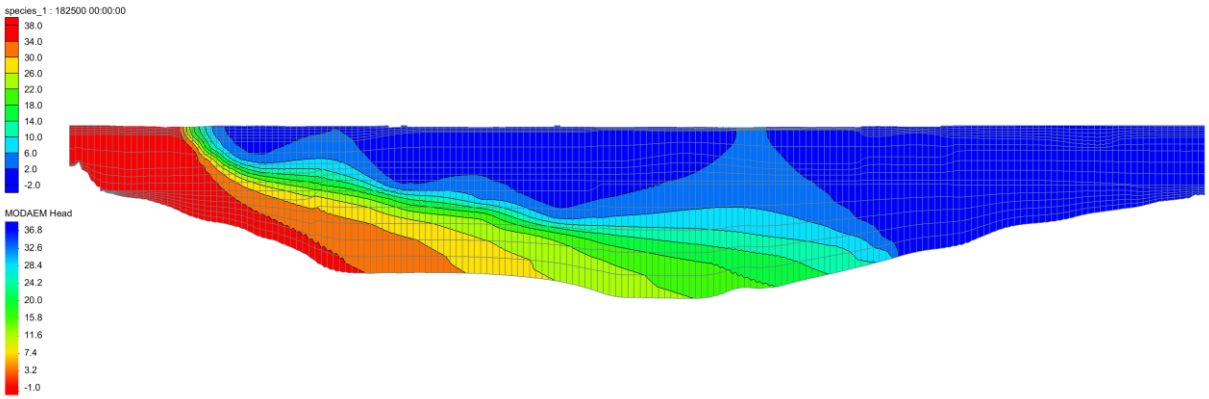

Figure 34 Cross-section of salinity field for winter period

Figure 35, Figure 36 and Figure 37 show transport steady state results for summer period. Sources of salt water were sea and River Neretva up to Opuzen with concentration of 36 g/l. Impact of channel Jasenska and Mala Neretva in mitigation of salt water intrusion is noticed in all layer due to increase of hydraulic conductivity in the layer of clay.

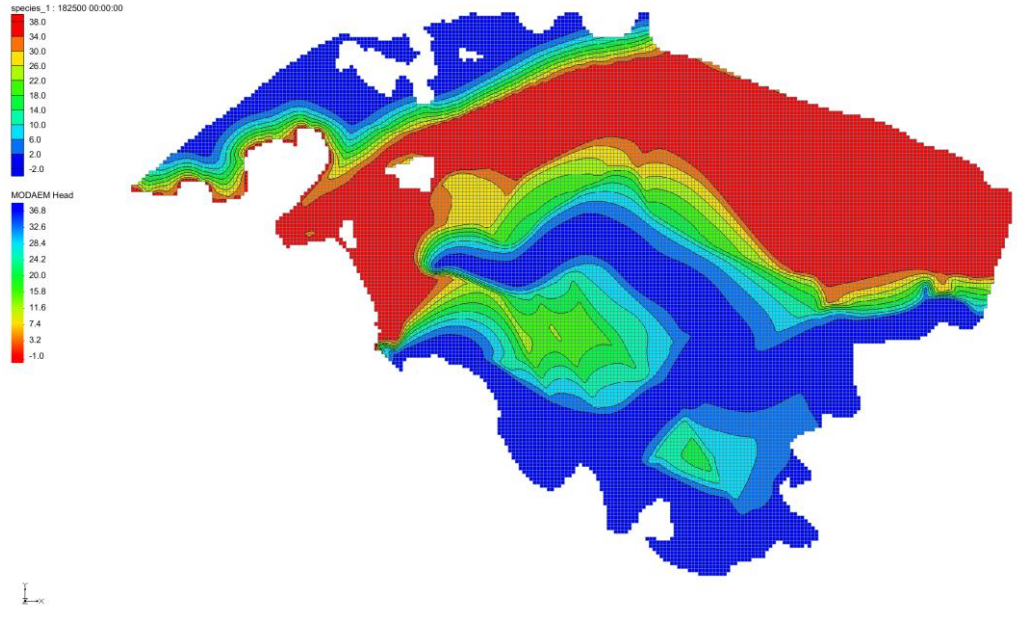

Figure 35 Salinity field for summer period in surface layer

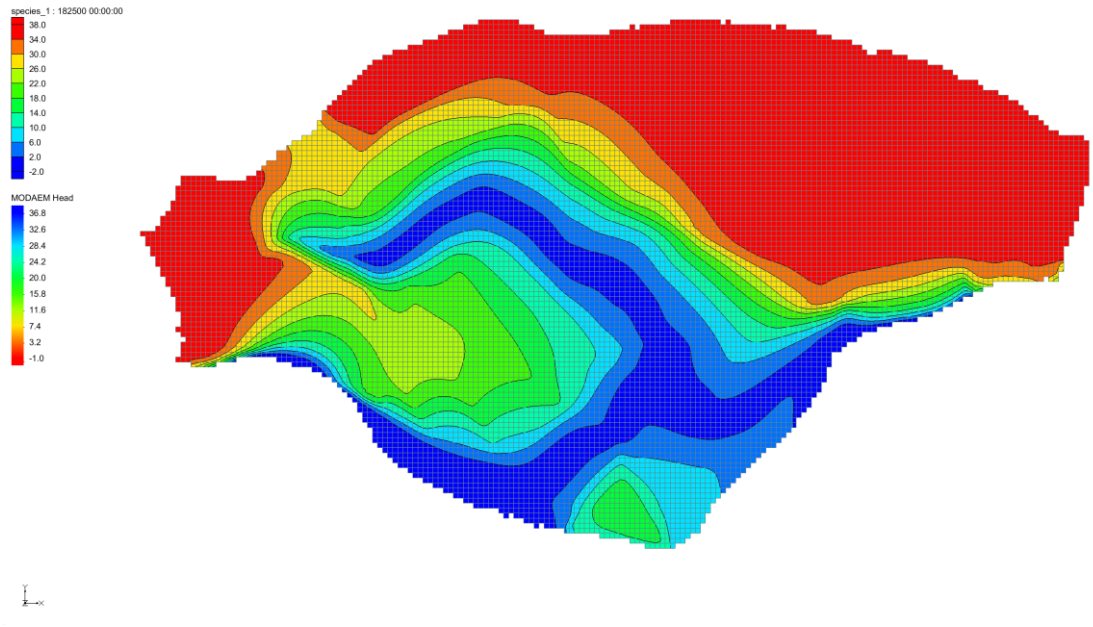

Figure 36 Salinity field for summer period in gravel layer

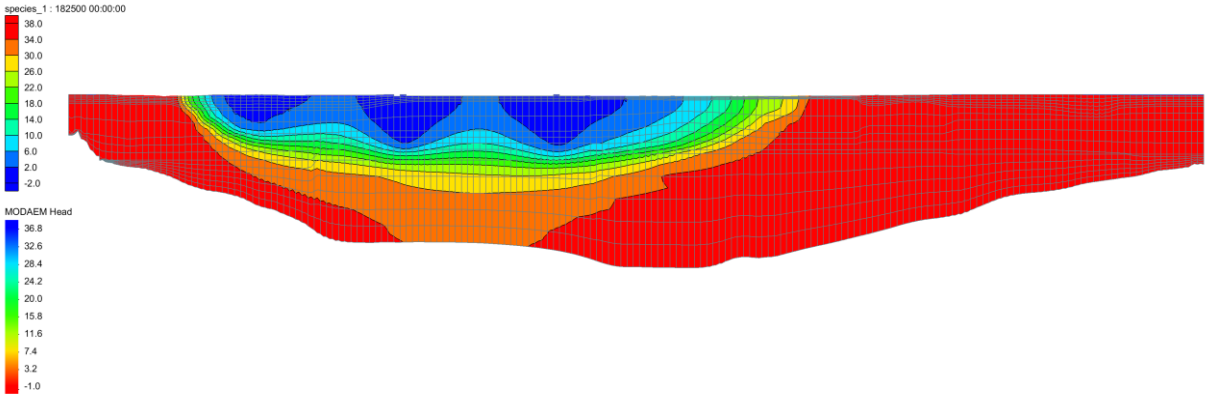

Figure 37 Cross-section of salinity field for summer period

From the spatial distribution of the salinity in the model it was possible to conclude that summer period is untoward period for the model. Concentration values are higher in the whole area of the model and larger area of the model is influenced by saltwater intrusion. Due to that, summer period is taken as relevant period of the year for further modelling.

Calibration and model results

Flow steady state results

After starting flow steady state simulation preliminary results were obtained. Figure 38 shows head values on surface layer and it is possible to see great impact of drain channels on lowering head values on the surface of the model in the middle of River Neretva Valley and southeast from Mala Neretva. Head values are in interval between 0.71 and -2.88 m. Highest head values are around River Neretva, Mala Neretva and channel Crepina and the lowest values are around channel Jasenska and in Luke area.

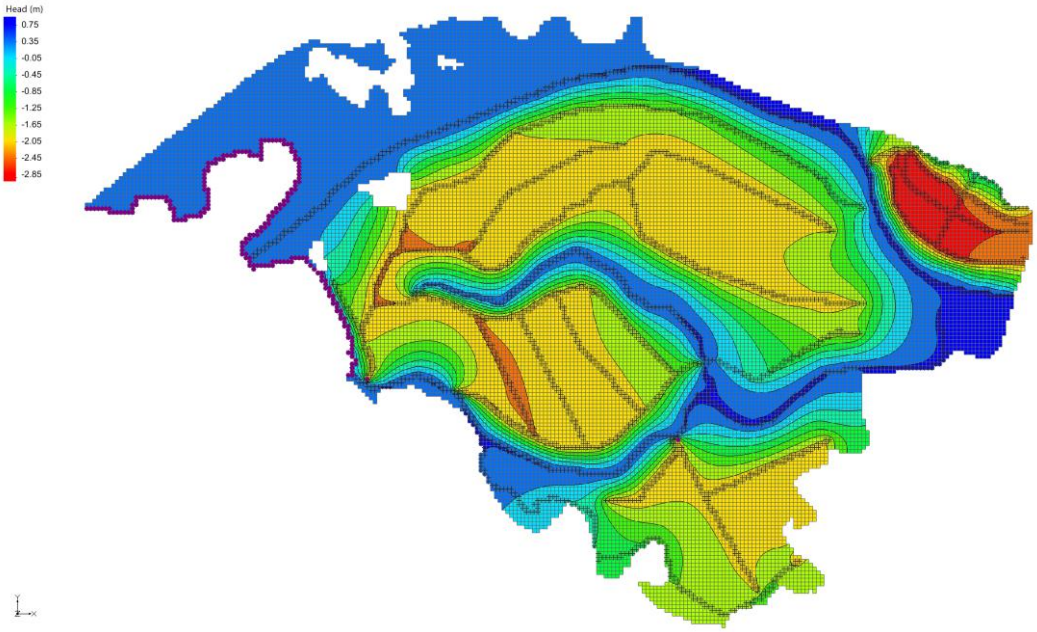

Figure 38 Steady state head results for surface layer

Figure 39 shows head values for flow steady state simulation in the layer of gravel on average depth of 40 m. There is no influence of drain channels in layers below the layer of clay. Head values are in interval between 0.55 and 0.2 m and are under main influence of CHD sea boundary condition and specified flow (Opuzen boundary condition).

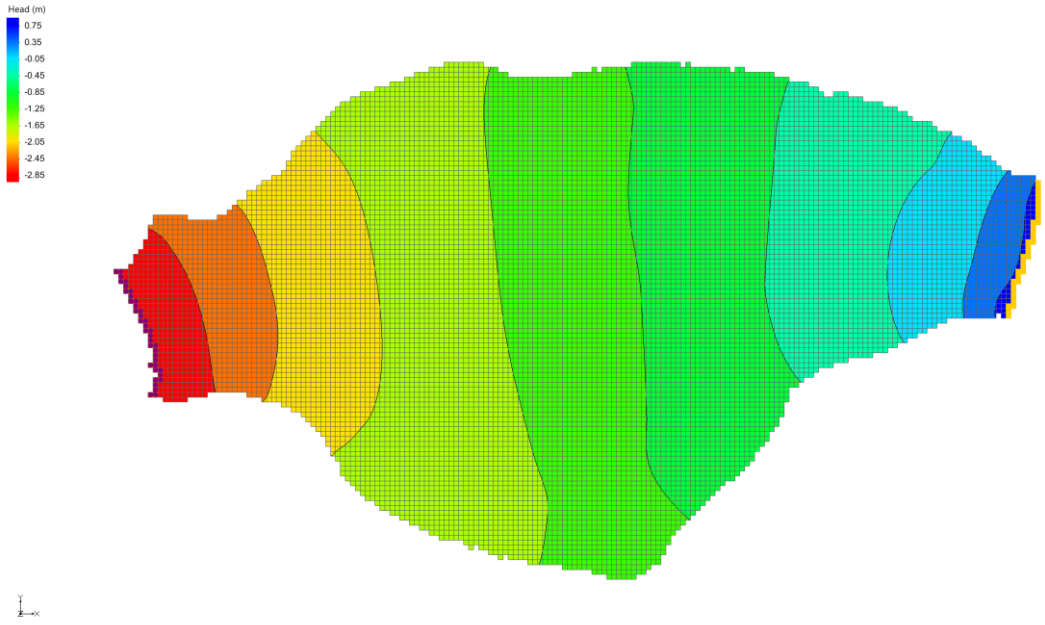

Figure 39 Steady state head results for the layer of gravel

Transient flow results

Measurements from tide gauge and limnigraph were taken as time variant head boundary condition for seawater and River Neretva. Opuzen boundary condition was defined as time variant specified flow. Head values from pumping stations Prag-Vidrice and Modrič were taken as time variant head boundary for Mala Neretva and channels.

Next figures are showing head results in specified times of simulation. Data range is the same for all figures. In the layer of sand, the changes are too small to notice on the figures.

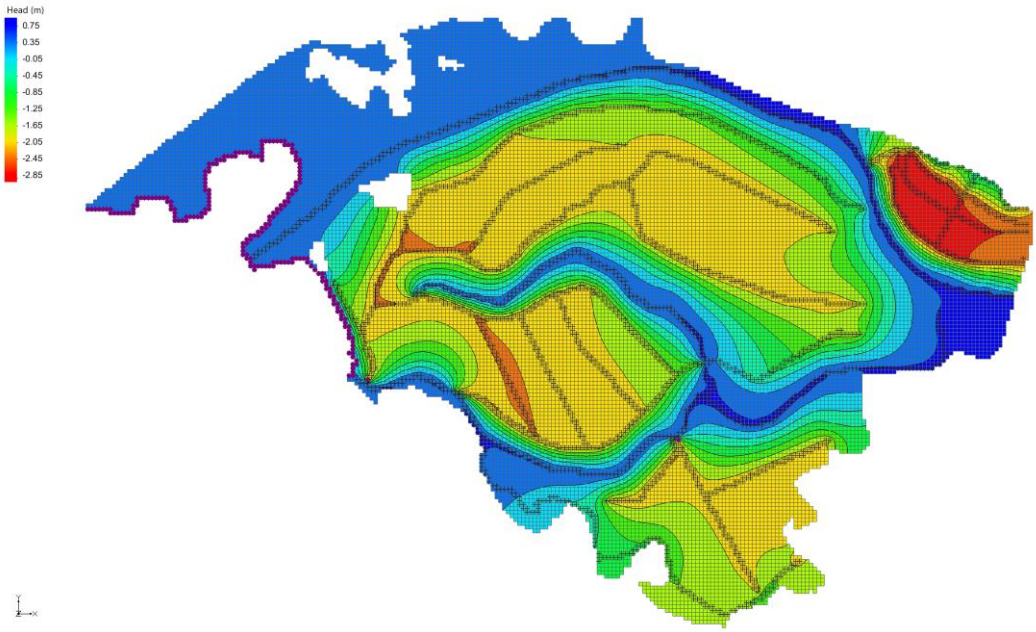

Figure 40 Head results in sand layer after 1 h for transient flow simulation

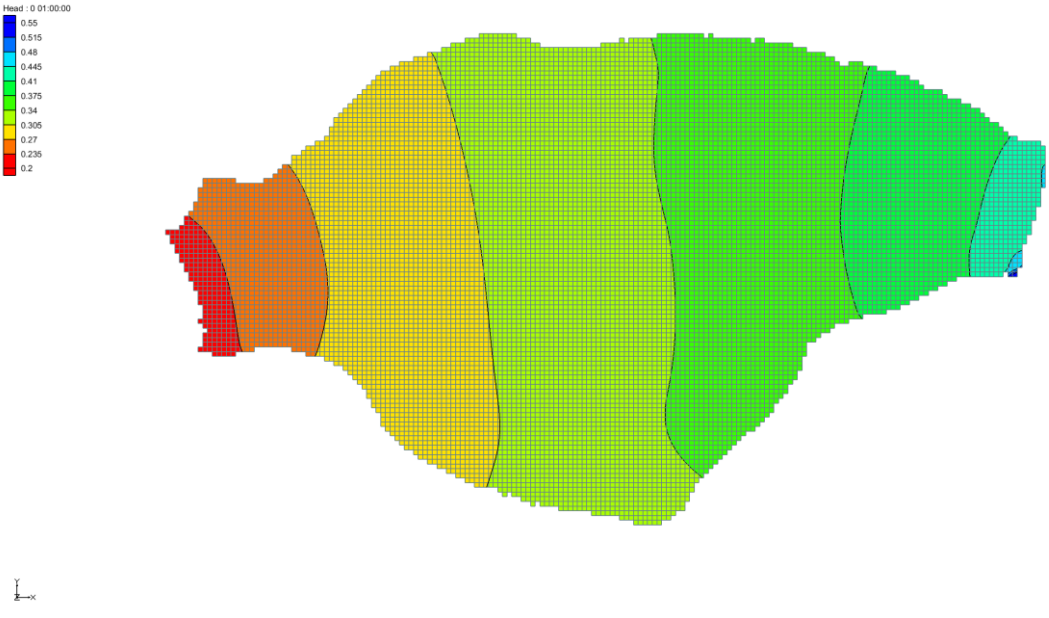

Figure 41 Head results in the layer of gravel after 1 h for transient flow simulation

Figure 42 Head results in the layer of gravel after 8 h for transient flow simulation

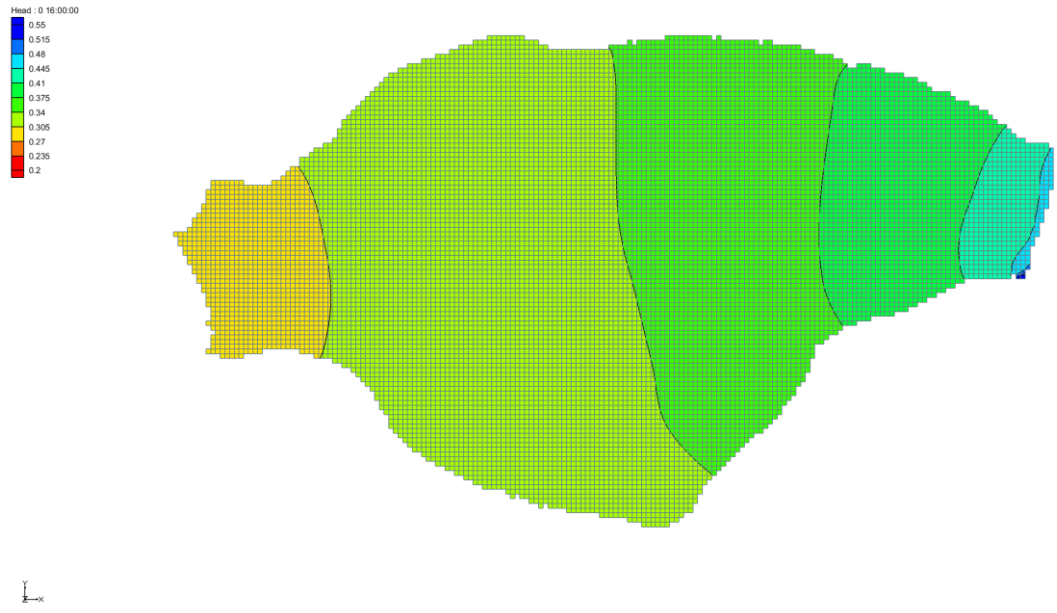

Figure 43 Head results in the layer of gravel after 16 h for transient flow simulation

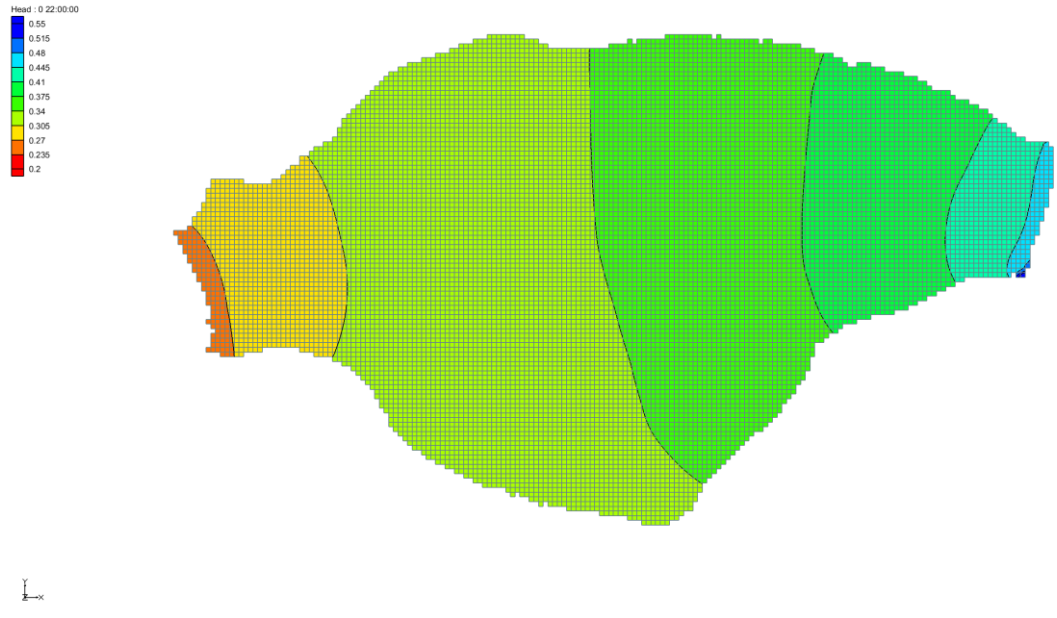

Figure 44 Head results in the layer of gravel after 22 h for transient flow simulation

Flow and transport steady state results

For this model flow and transport steady state simulation was set as transient simulation with transient constant boundary conditions. It was accepted as steady state simulation if there were no changes in head or concentration values during the time. Simulation was set for the period of 500 years and it achieved steady state after approximately 250 years.

Flow boundary conditions for coupled steady state simulation were mean values of determined boundary condition values. Flow initial condition for coupled steady state simulation were head results of flow steady state simulation.

Transport boundary conditions for coupled steady state simulation was concentration value of 36 g/l along the sea line and in all layers for River Neretva. Boundary conditions for Opuzen, Mala Neretva and channels were defined as $dC/cX \neq 0$, $dC/dZ \neq 0$. Transport initial condition for coupled steady state simulation was concentration value of 0 g/l for the whole area of the model.

For flow and transport steady state simulation the value of hydraulic conductivity for the layer of clay was set on the value 10^{-5} m/s. Only with this modification achievement of steady state was possible.

Figure 45 shows head results for surface layer for flow and transport steady state simulation. Just like for the results of flow steady state simulation, it is possible to see great impact of drain channels on lowering head values on the surface of the model in the middle of River Neretva Valley and southeast from Mala Neretva. Head values are in interval between 0.5 and -2.8 m.

Figure 46 shows head results for layer of gravel for flow and transport steady state simulation. It is possible to notice difference between head results for layer of gravel for flow steady state simulation and coupled steady state simulation. This difference is due to increase the value of hydraulic conductivity for the layer of clay. Head values are in interval between 0.23 and -1.1 m and are under low influence of drain channel due to permeability of layer of clay.

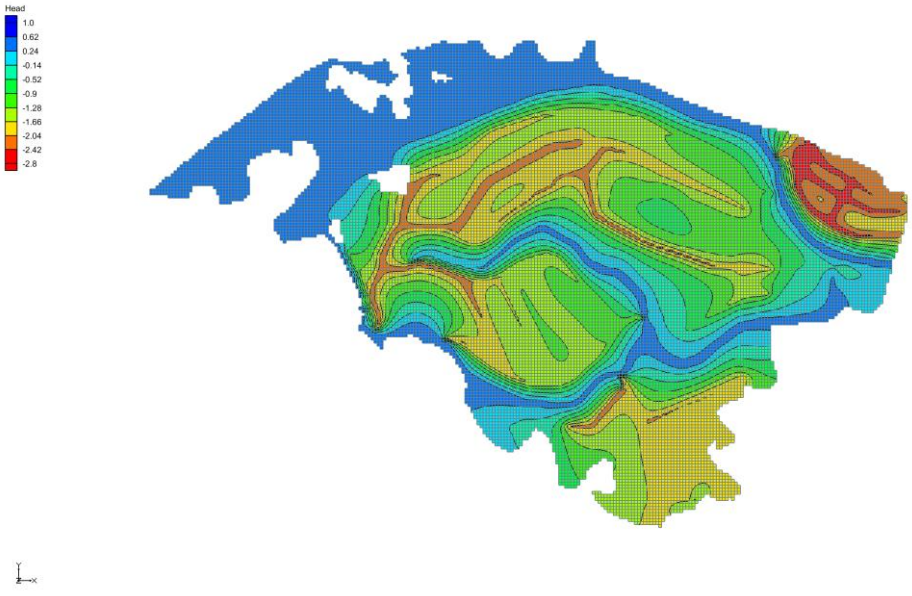

Figure 45 Head results for surface layer for flow and transport steady state simulation

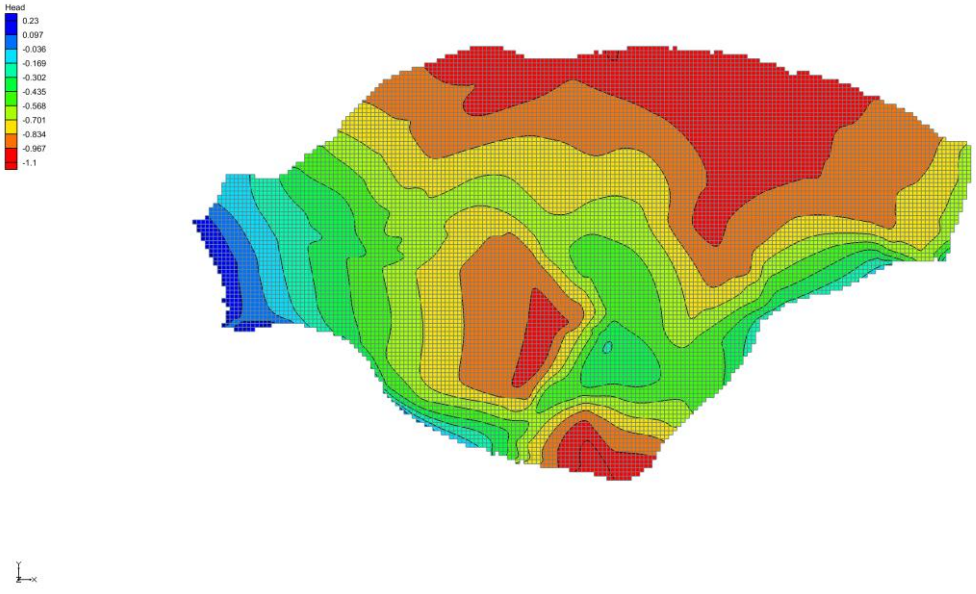

Figure 46 Head results for gravel layer for flow and transport steady state simulation

Figure 47 shows concentration values for surface layer for flow and transport steady state simulation. Sea and River Neretva are source of salt water intrusion and the area around them have the highest value of concentration. Mala Neretva and channel Crepina have the lowest values of concentration in the model.

Figure 48 shows concentration values for layer of gravel for flow and transport steady state simulation. Sea is the only real source of salt water but since the hydraulic conductivity for the layer of clay was increased there is salt water intrusion from upper layers of the model.

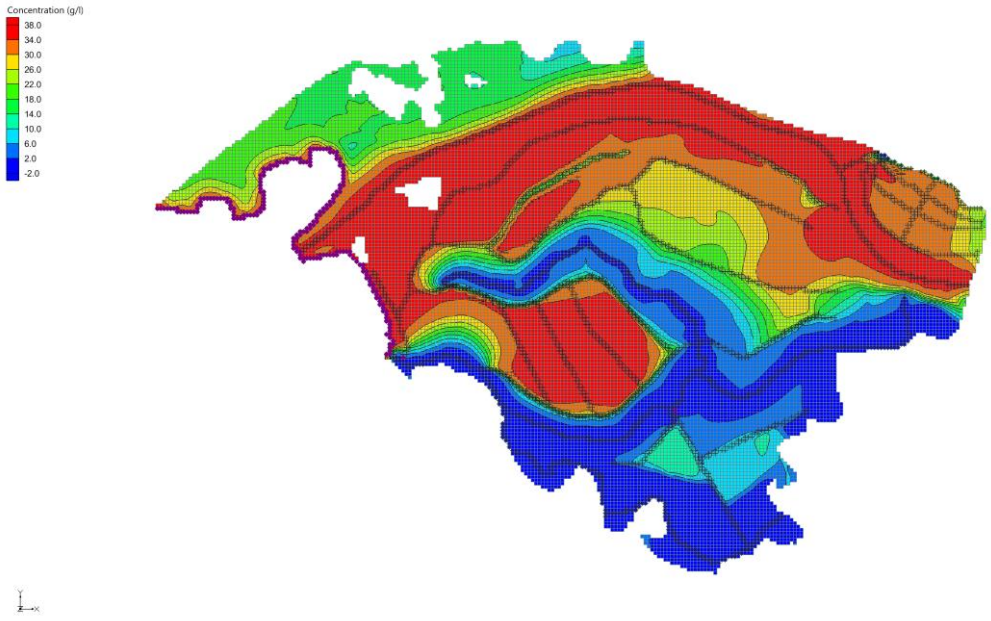

Figure 47 Transport results for surface layer for flow and transport steady state simulation

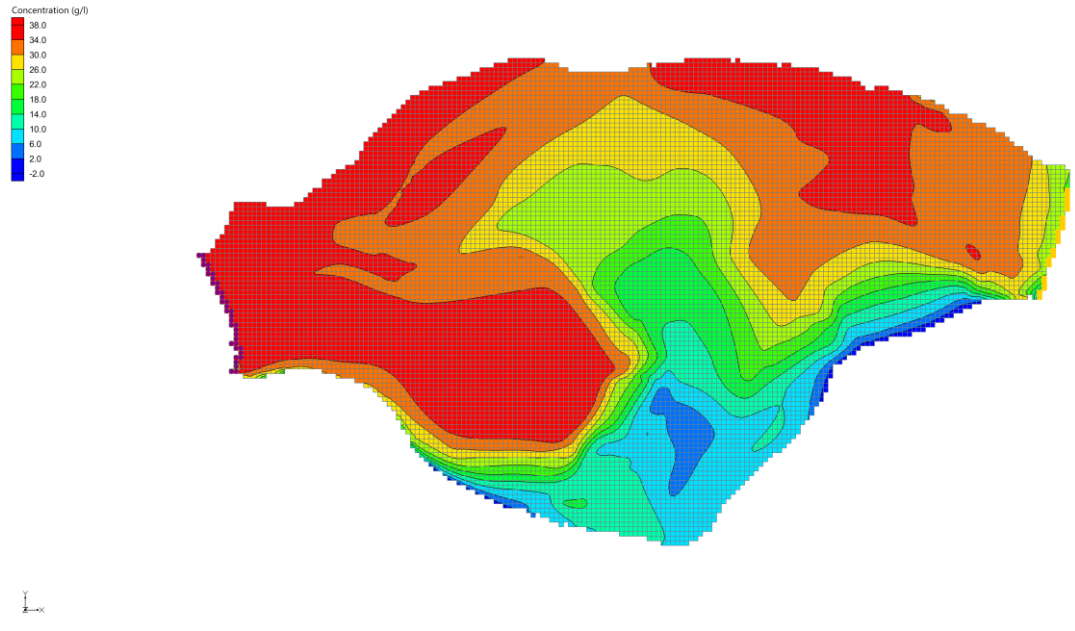

Figure 48 Transport results for layer of gravel for flow and transport steady state simulation

Most important output from flow and transport steady state simulation was the field of salinity that is initial condition for flow and transport transient simulation. Values of concentration gained from flow and transport steady state simulation correspond to the mean values of concentration of measured data.

Table 1 Measured and modelled values of concentration for all piezometers

SAMPLING LOCATION	Measured mean value of concentration (g/l)	Modeled mean value of concentration (g/l)
P1	32.56	36.0
P2	27.37	31.4
P4	1.13	0.29
D1	36.0	35.2
D2	21.25	30.9
D3	25.15	29.8
D4	14.13	10.25

Transient flow and transport transient results

Last step of model was to obtain transient flow and transport simulation. Simulation is created for the period of one month and all data that was used present measured values for July 2021.

Flow boundary conditions for transient flow and transport simulations were time variant values of determined boundary condition. Values of all boundary conditions were set for 744 hours. Flow initial condition for transient flow and transport simulation were head results of flow steady state simulation.

Transport boundary conditions for transient flow and transport simulation was the value of 36 g/l along the sea line and in River Neretva. Values of measured concentration were added for channels Jasenska, Modrič and Prag-Vidirice. Boundary conditions for Opuzen, Mala Neretva and the rest of the channels were defined as $dC/cX \neq 0$, $dC/dZ \neq 0$. Transport initial condition for transient flow and transport simulation were the values of concentration obtained in flow and transport steady state simulation.

For transient flow and transport simulation the value of hydraulic conductivity for the layer of clay was set on the value 10^{-8} m/s.

Recharge values were added in simulation.

Next figures show measured and modelled head values for July 2021 for all piezometers.

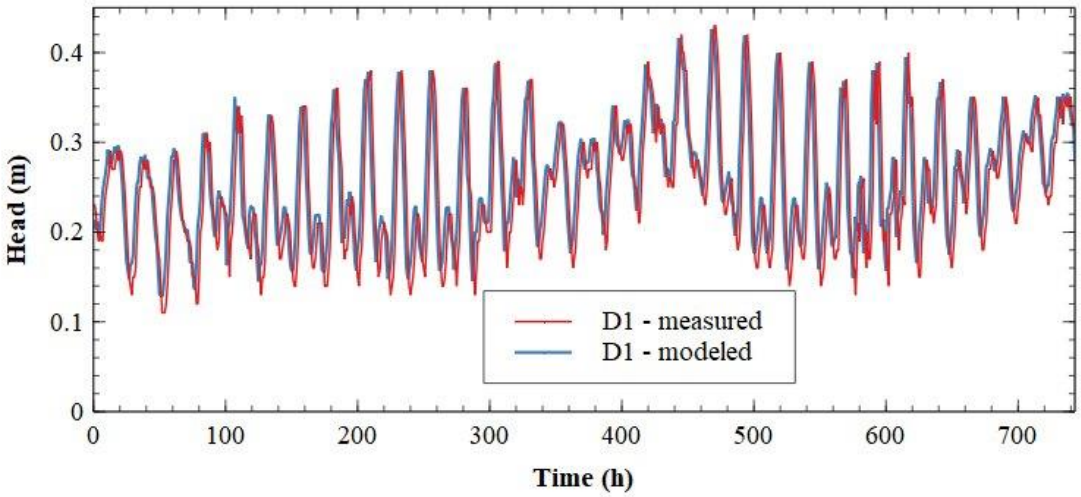

Figure 49 Measured and modelled head values for July 2021 on piezometer D1

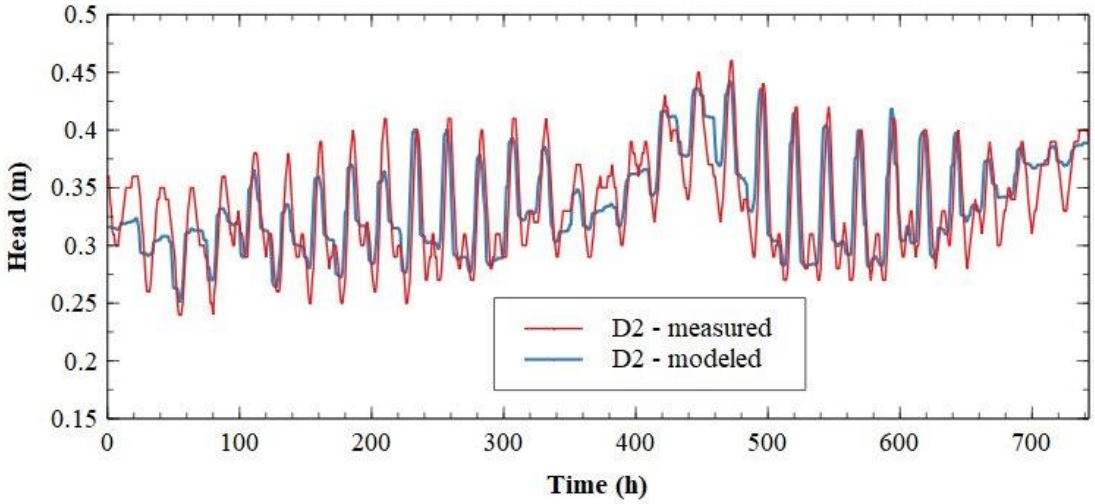

Figure 50 Measured and modelled head values for July 2021 on piezometer D2

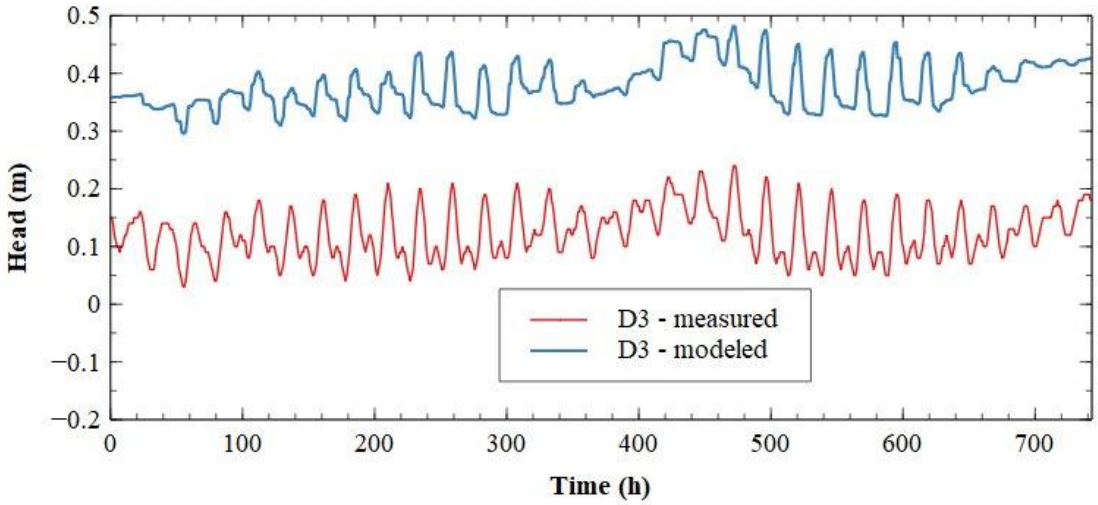

Figure 51 Measured and modelled head values for July 2021 on piezometer D3

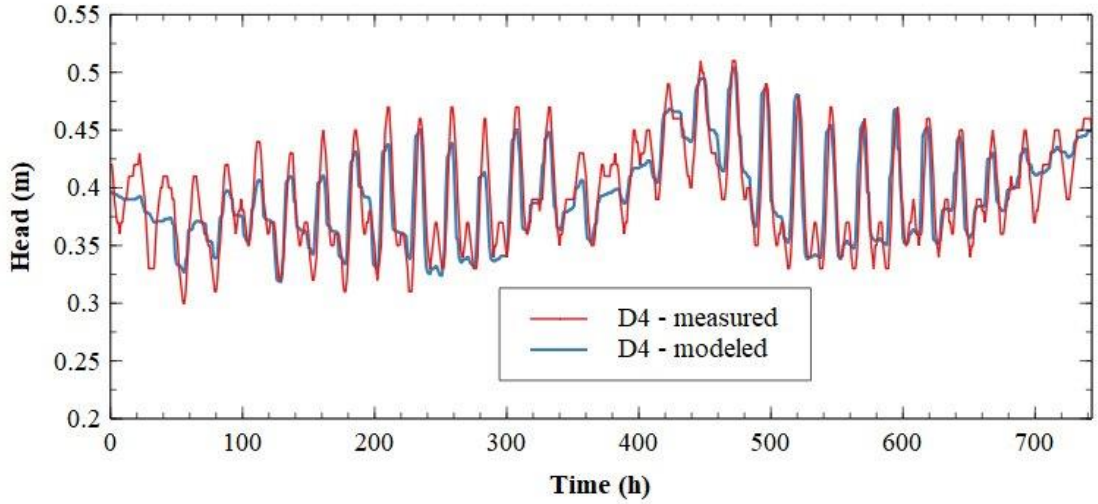

Figure 52 Measured and modelled head values for July 2021 on piezometer D4

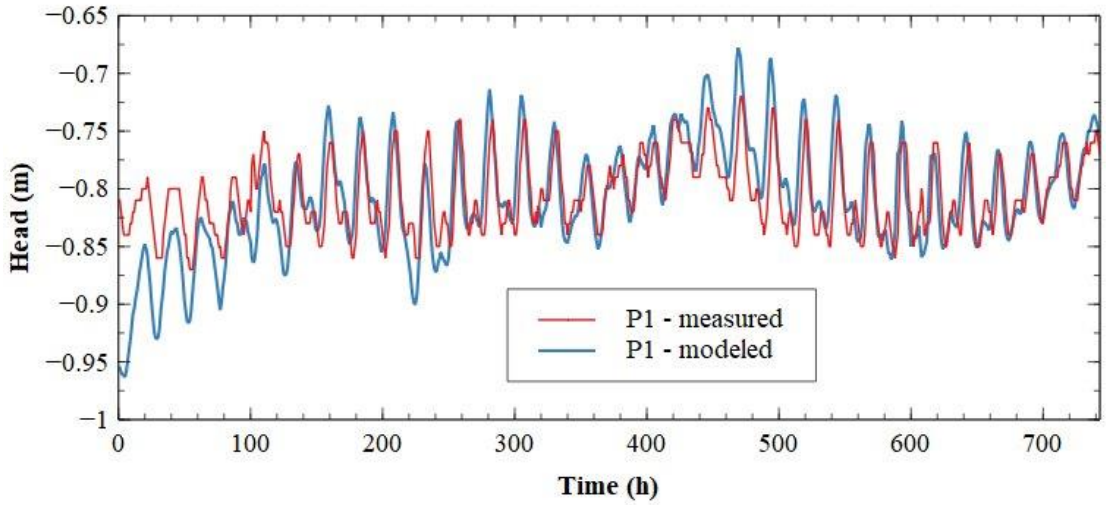

Figure 53 Measured and modelled head values for July 2021 on piezometer P1

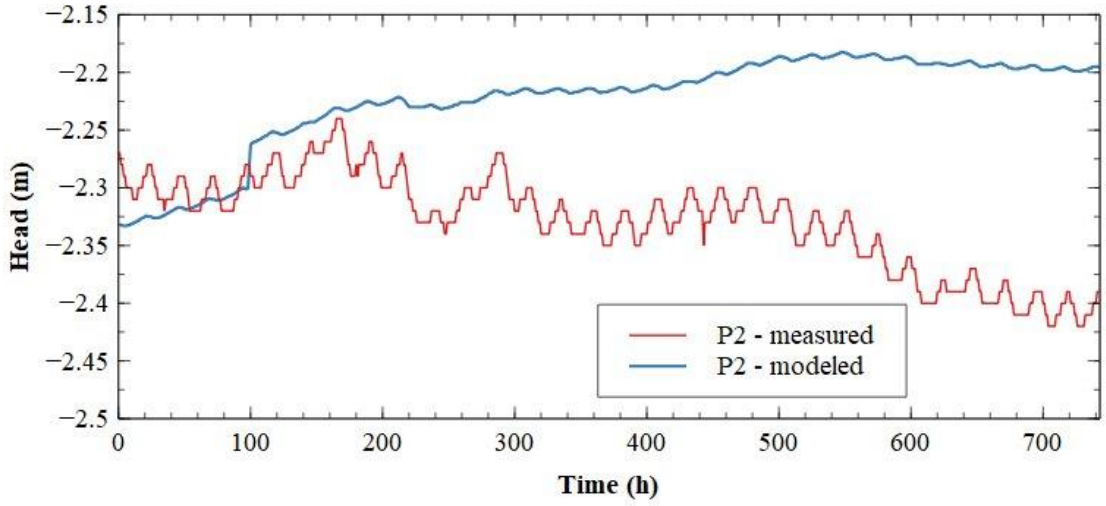

Figure 54 Measured and modelled head values for July 2021 on piezometer P2

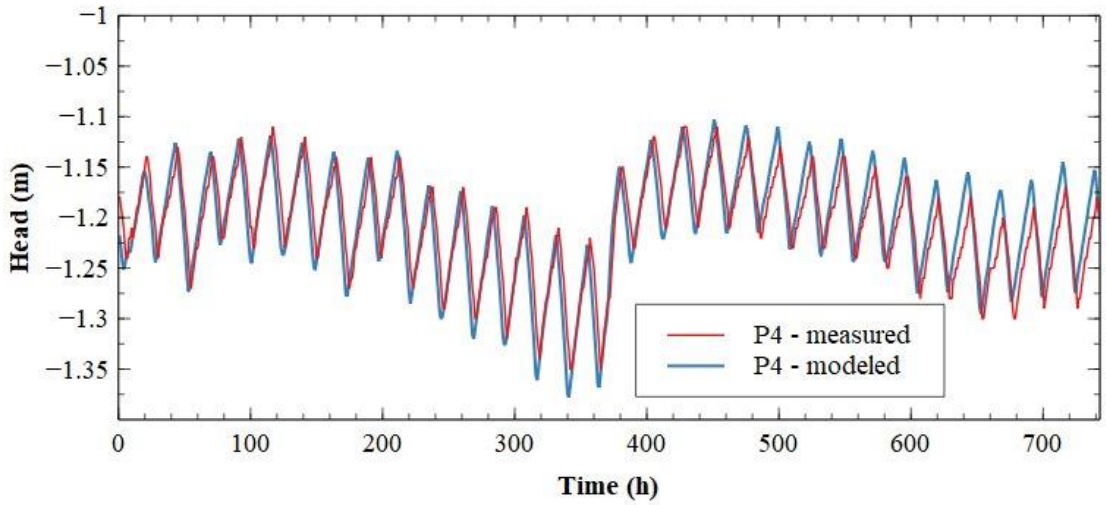

Figure 55 Measured and modelled head values for July 2021 on piezometer P4

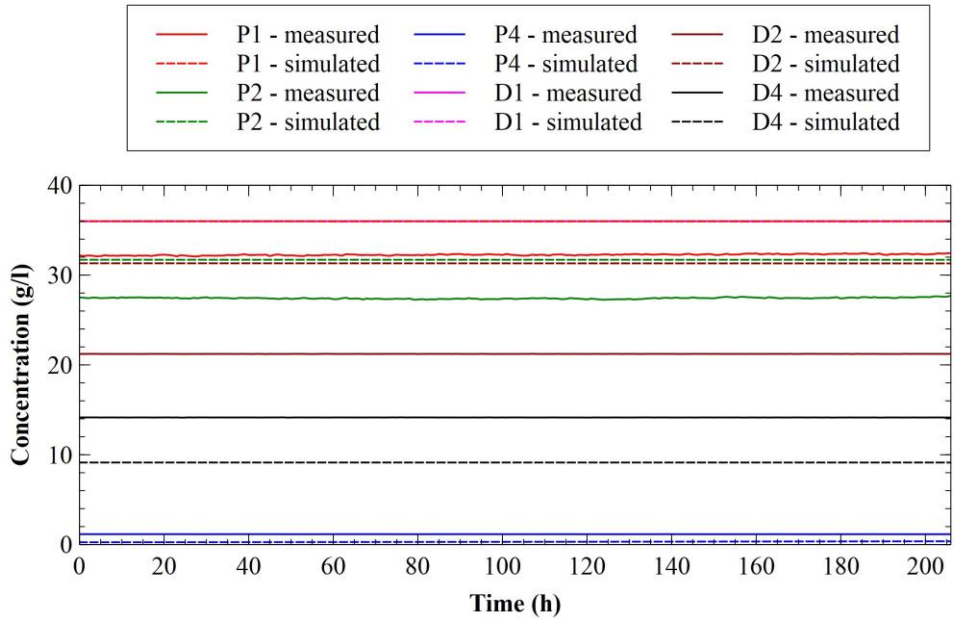

Figure 56 Measured and modelled concentration values for July 2021

Calibration of results and definition of final model parameters

After setting all four steps of the model preliminary results were obtained. Based on preliminary results model settings were changed to get a better match between measured and modelled values of head and concentration in all piezometers. All steps of model setup were repeated until best match was obtained.

Model parameters that were calibrated are the values of hydraulic conductivity for the layers of sand (model layers 1-5) and for the layers of gravel (model layers 8-16), channel conductance and specified flow.

For the initial values of hydraulic conductivity for each layer, average value from boreholes for that layer were taken. During the process of calibration, it is noticed that values of hydraulic conductivity are not distributed equally within a single layer.

For shallow piezometers calibration, horizontal hydraulic conductivity for the layer of sand and channel conductance were calibrated to get better match between measured and modelled values.

Adopted values of horizontal hydraulic conductivity are shown on Figure 57. It is possible to notice that the whole area of the layer of sand have the value of horizontal hydraulic conductivity of 1.8 m/h (0.0005 m/s) and that only the area of Diga have higher value of horizontal hydraulic conductivity that is 23 m/h (0.0064 m/s). The reason for this exception is that the area of Diga is an embankment that is constructed with bulk material that differs from the material from the rest of the valley.

After setting horizontal hydraulic conductivity for the layer of sand it was possible to notice influence of channel conductance on head values in shallow piezometers. On piezometar P1 the greatest influence has channel parallel with Diga embankment and it lowers the mean value of head in P1 that is dominantly influenced by the sea level. On piezometar P2 the greatest influence has channel Jasenska and nearby channels. Conductance for all channels was adapted to get best matching between measured and modelled values. On piezometar P4 the greatest influence has pumping station Prag-Vidice and two channels south from Mala Neretva.

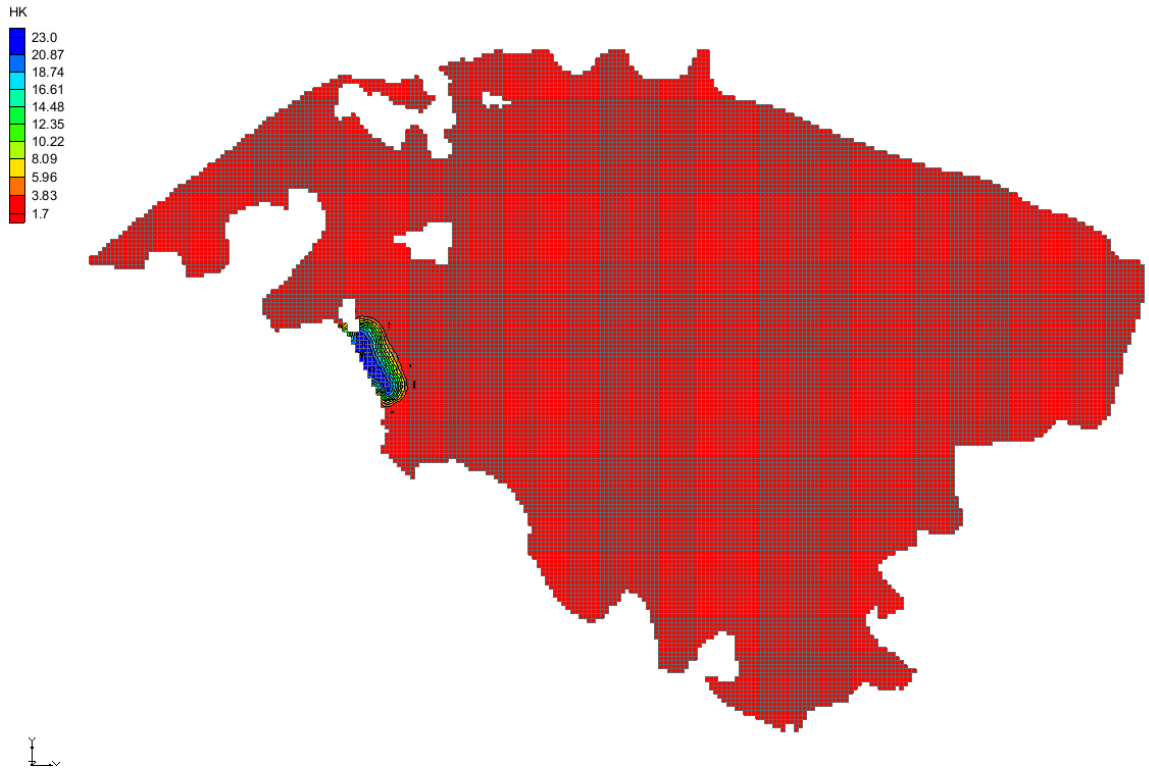

Figure 57 Adopted horizontal hydraulic conductivity values for the layer of sand

For deep piezometers calibration, horizontal hydraulic conductivity for the layer of gravel and specified flow were calibrated to get better match between measured and modelled values.

Adopted values od horizontal hydraulic conductivity are shown on Figure 58. North part of the layer of sand has the highest value of horizontal hydraulic conductivity with a value of 70 m/h (0.02 m/s). The value horizontal hydraulic conductivity declines toward south part of the layer of gravel. Lowest value horizontal hydraulic conductivity for the layer of gravel is 1.2 m/h (0.0003 m/s) and is located below the area of Vidrice.

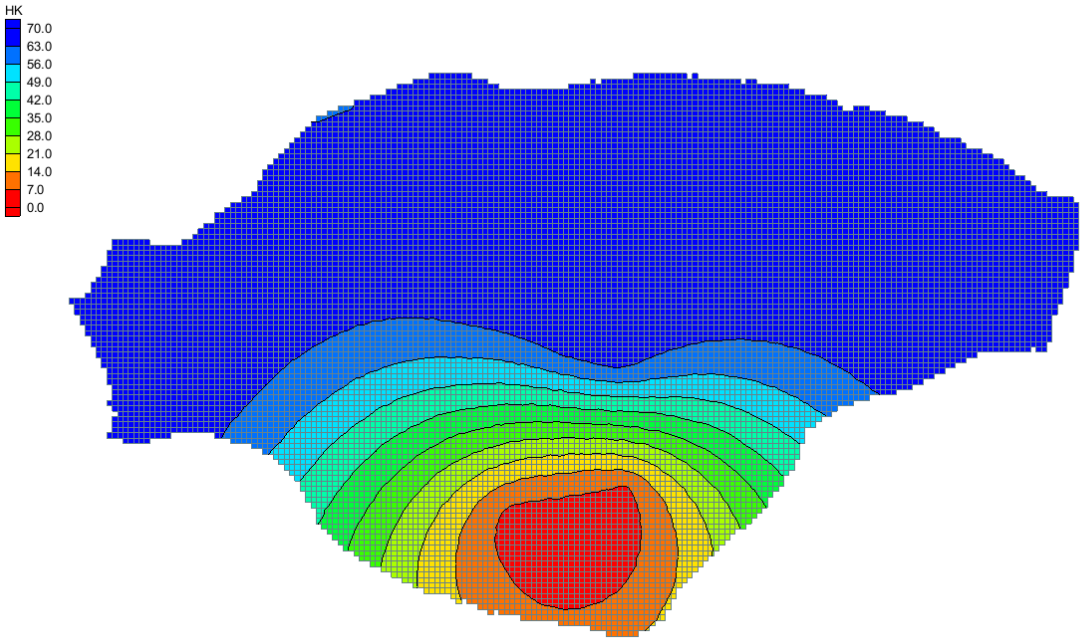

Figure 58 Adopted horizontal hydraulic conductivity values for the layer of gravel

Specified flow in the layer of gravel was determined based on adopted values of horizontal hydraulic conductivity and best matching of tidal efficacy and mean value between measured and modelled head values for deep piezometers. Figure 59 and Figure 60 show the relation between specified flow, horizontal hydraulic conductivity and tidal efficacy or mean head value.

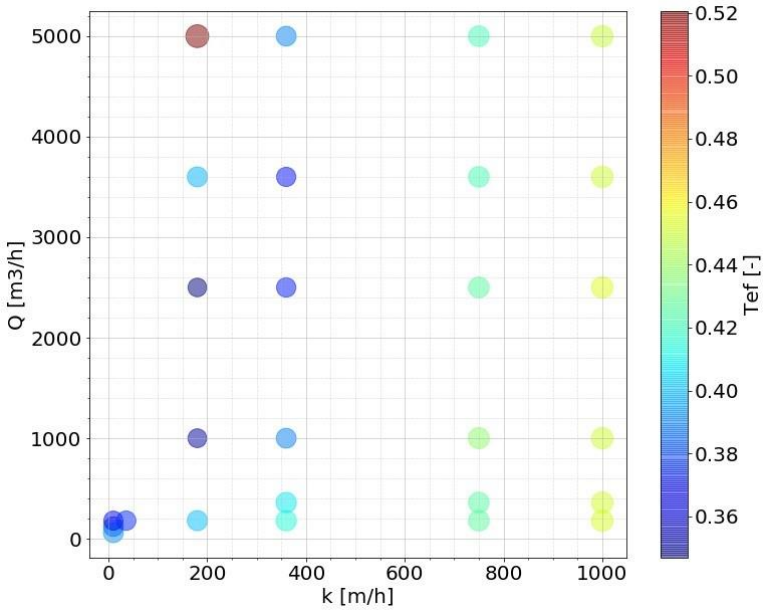

Figure 59 Relation between specified flow, horizontal hydraulic conductivity and tidal efficacy for deep piezometers

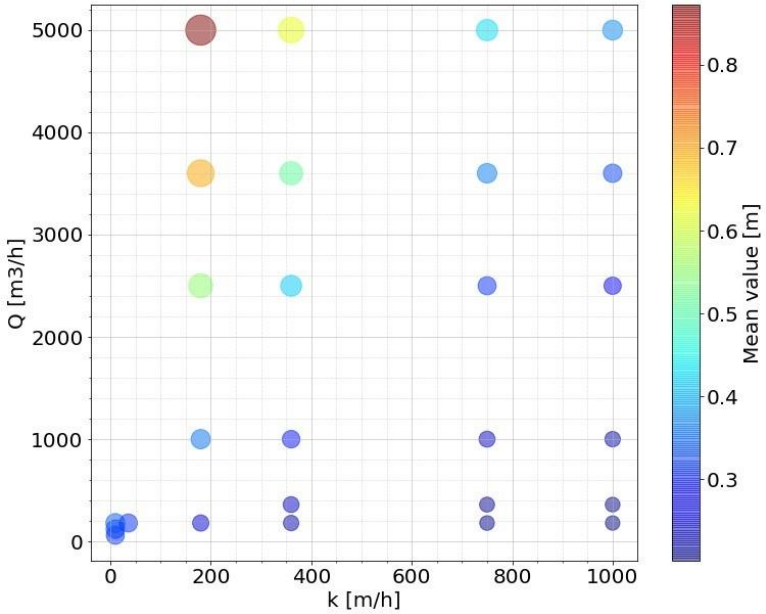

Figure 60 Relation between specified flow, horizontal hydraulic conductivity and mean head value for deep piezometers

Results verification

After getting calibrated results for July 2021 and defining all model parameters, verification of the results was carried out. For verification of the results all adopted model parameters were used while the boundary conditions were set separately for two periods, August and September 2021. All results are shown on figures below.

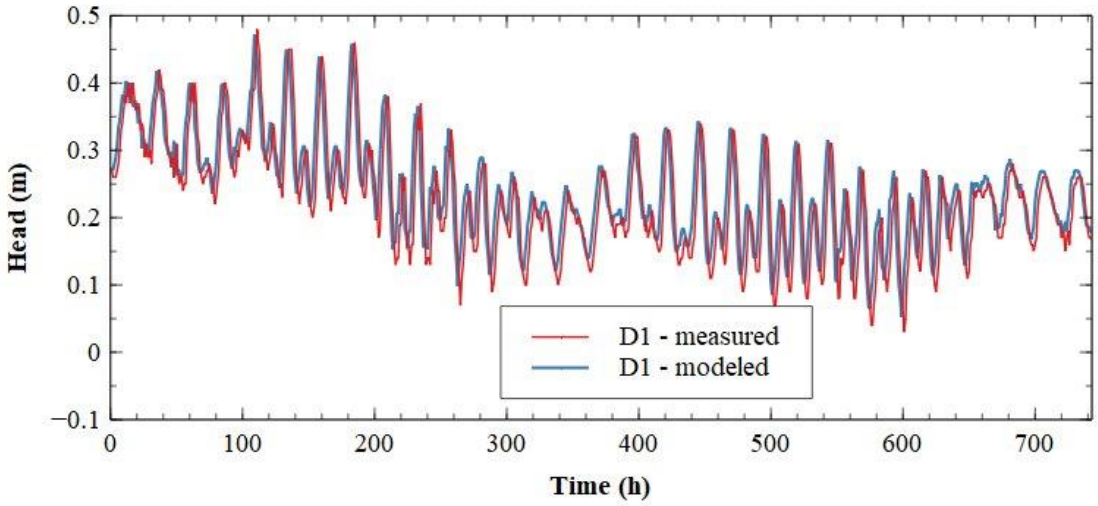

Figure 61 Measured and modelled head values for August 2021 on piezometer D1

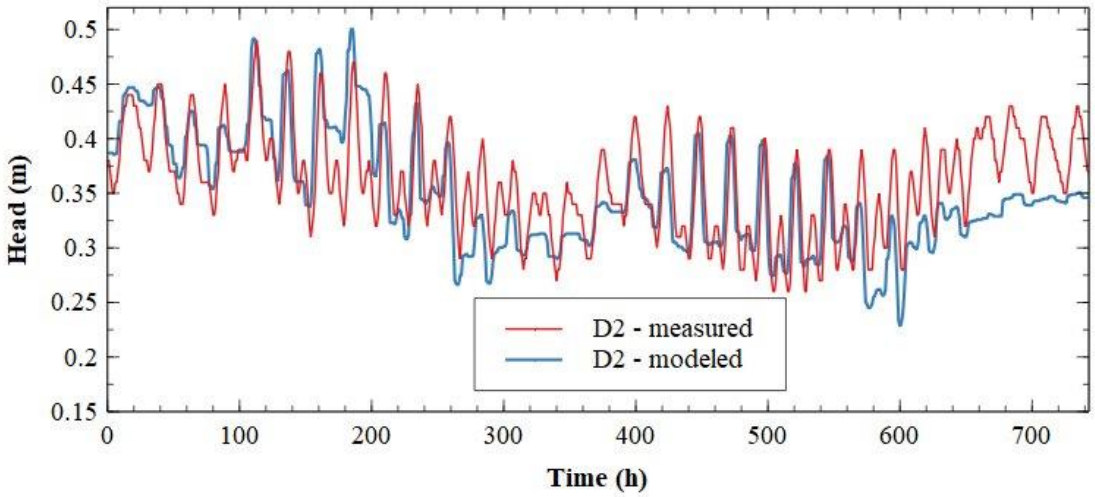

Figure 62 Measured and modelled head values for August 2021 on piezometer D2

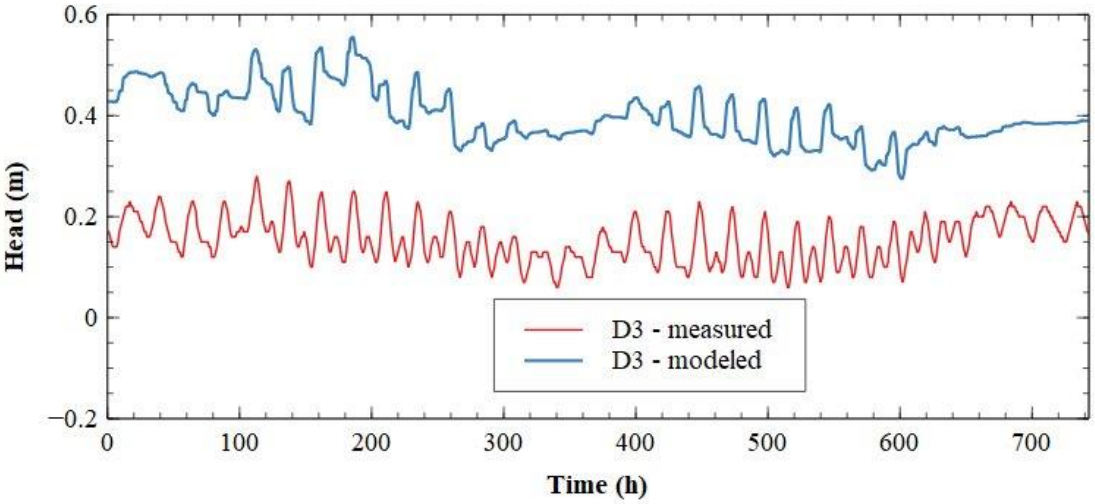

Figure 63 Measured and modelled head values for August 2021 on piezometer D3

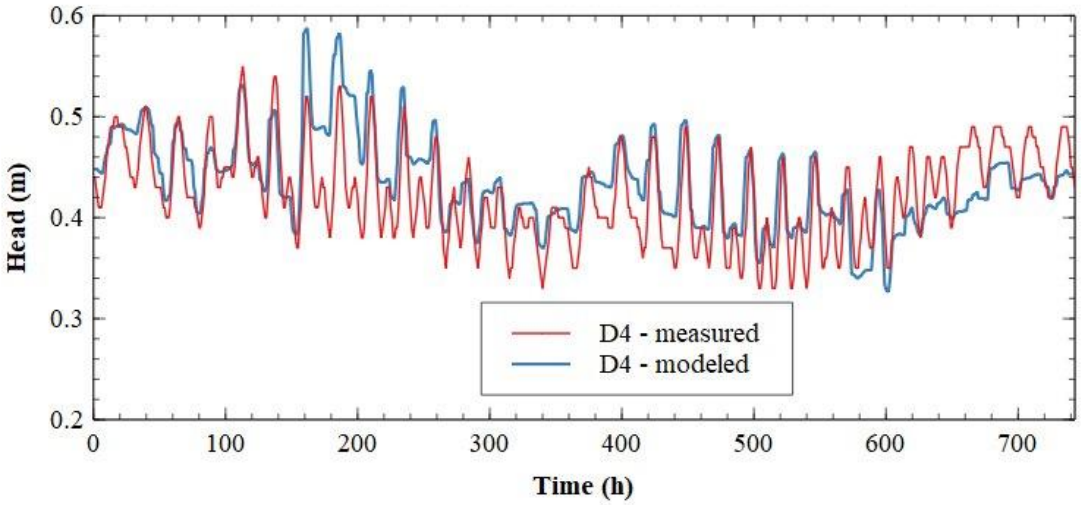

Figure 64 Measured and modelled head values for August 2021 on piezometer D4

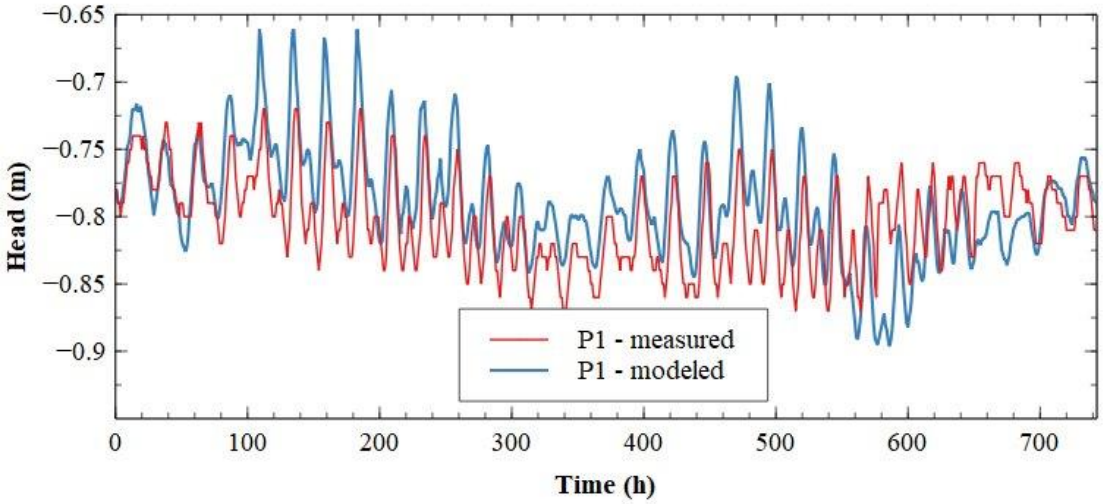

Figure 65 Measured and modelled head values for August 2021 on piezometer P1

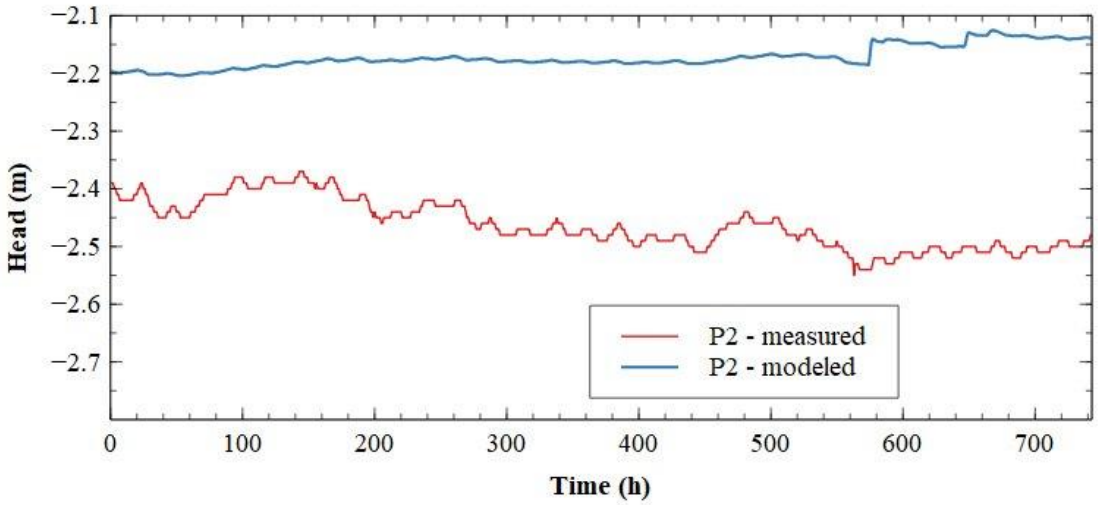

Figure 66 Measured and modelled head values for August 2021 on piezometer P2

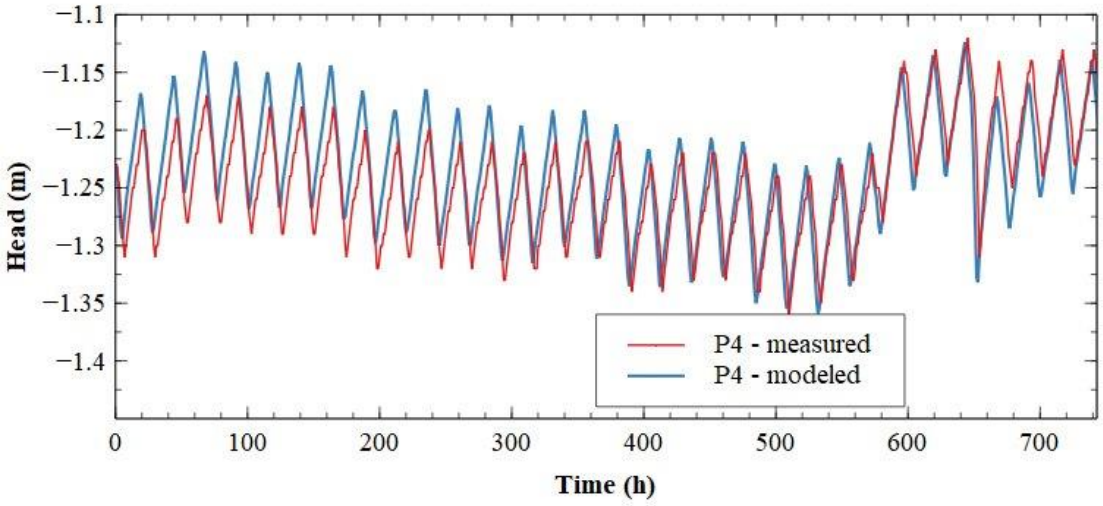

Figure 67 Measured and modelled head values for August 2021 on piezometer P4

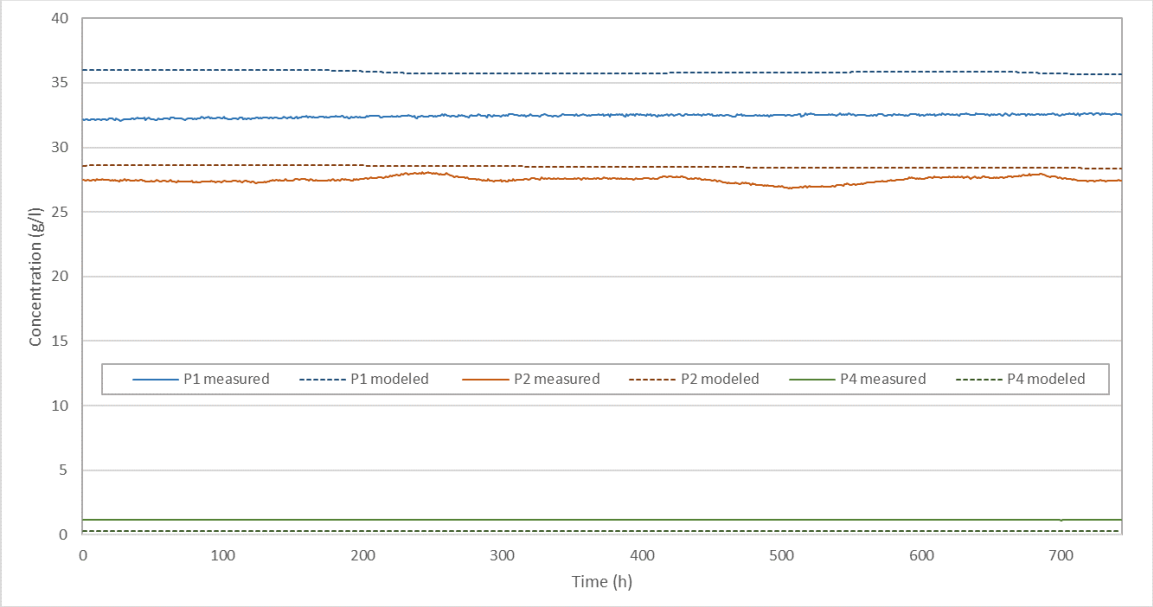

Figure 68 Measured and modelled concentration values for August 2021 on piezometers P1, P2 and P4

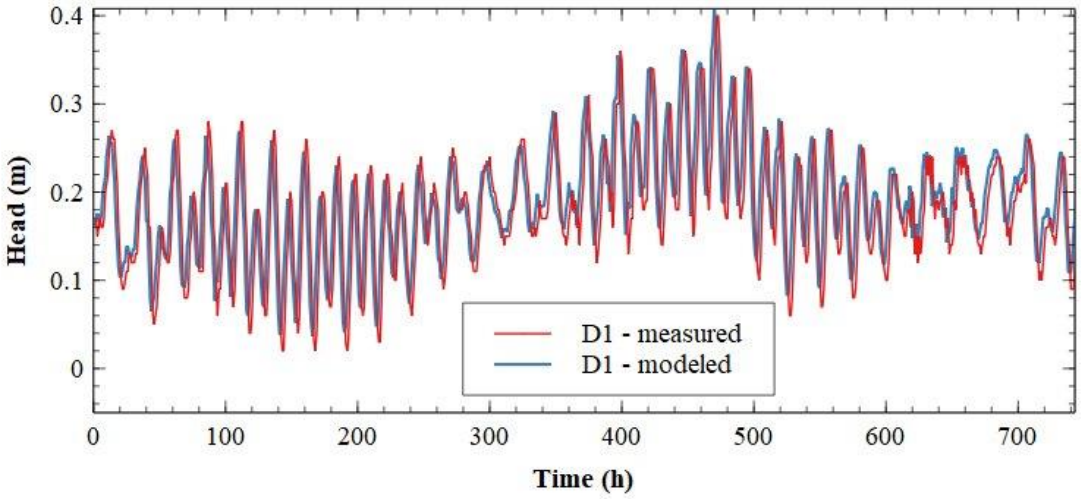

Figure 69 Measured and modelled head values for September 2021 on piezometer D1

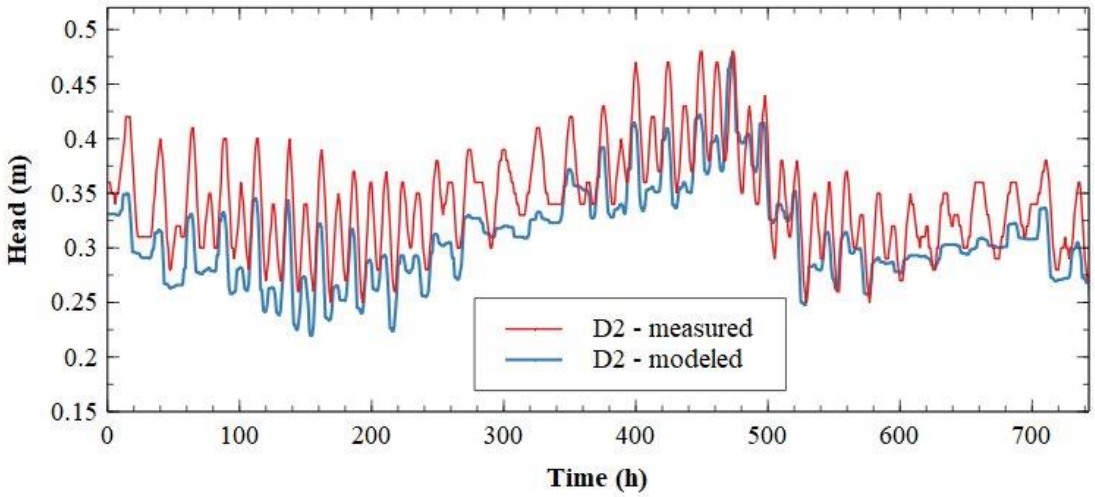

Figure 70 Measured and modelled head values for September 2021 on piezometer D2

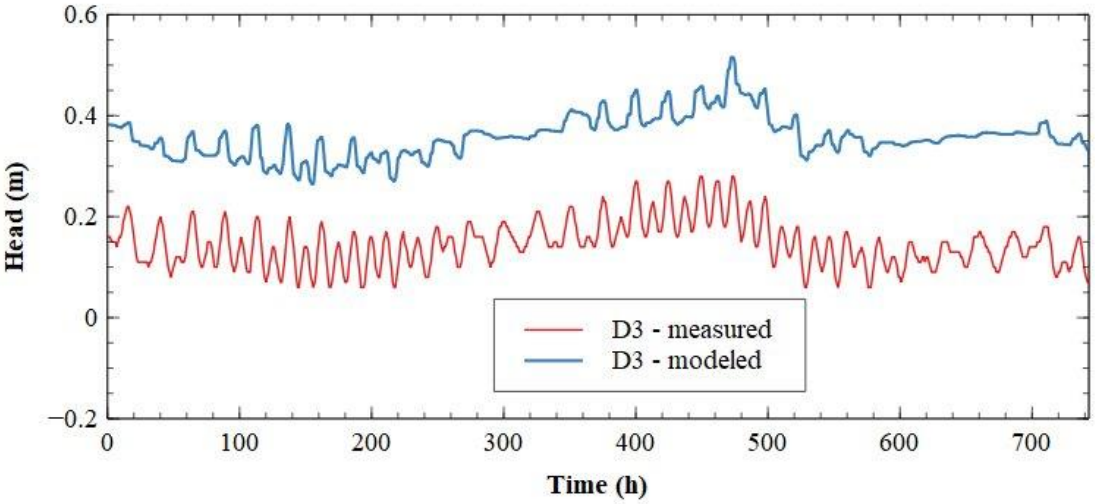

Figure 71 Measured and modelled head values for September 2021 on piezometer D3

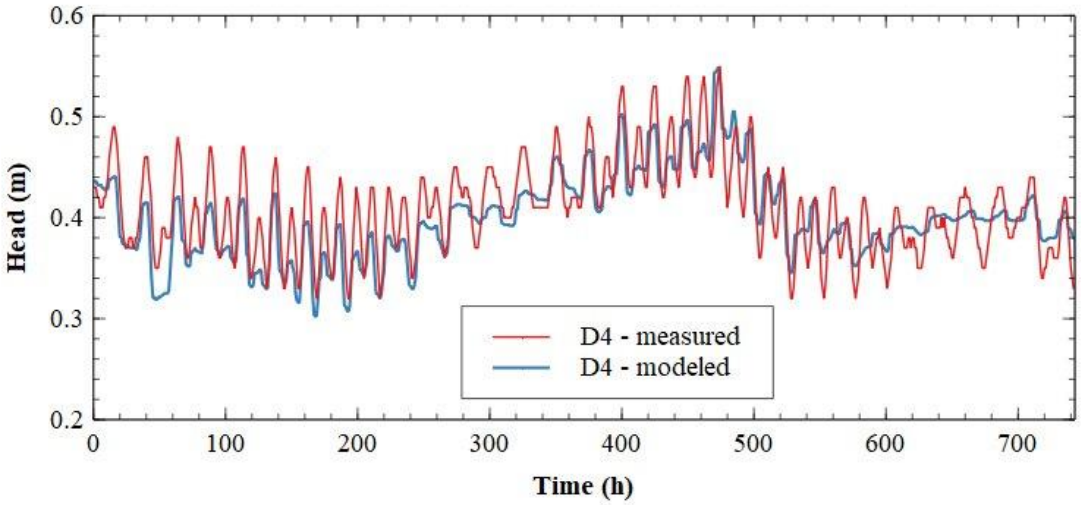

Figure 72 Measured and modelled head values for September 2021 on piezometer D4

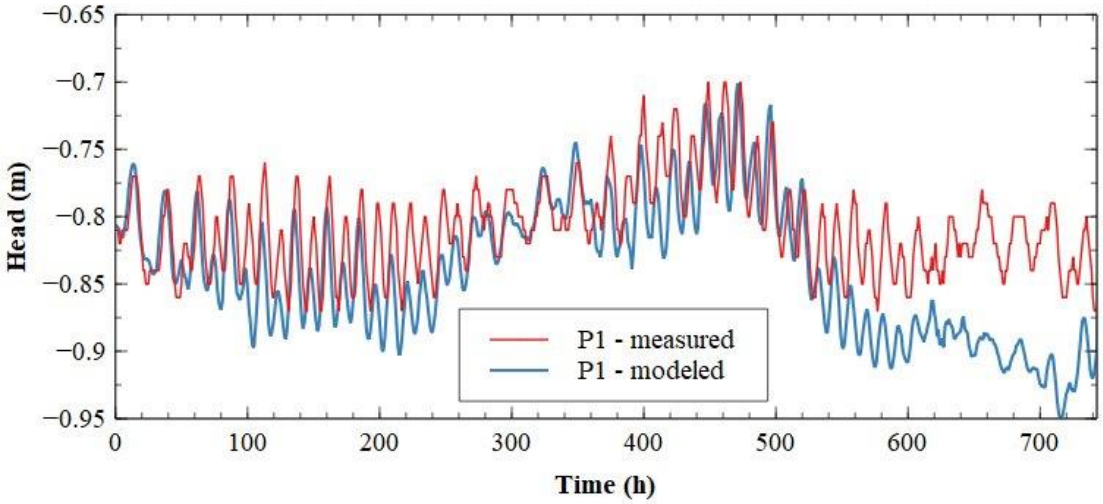

Figure 73 Measured and modelled head values for September 2021 on piezometer P1

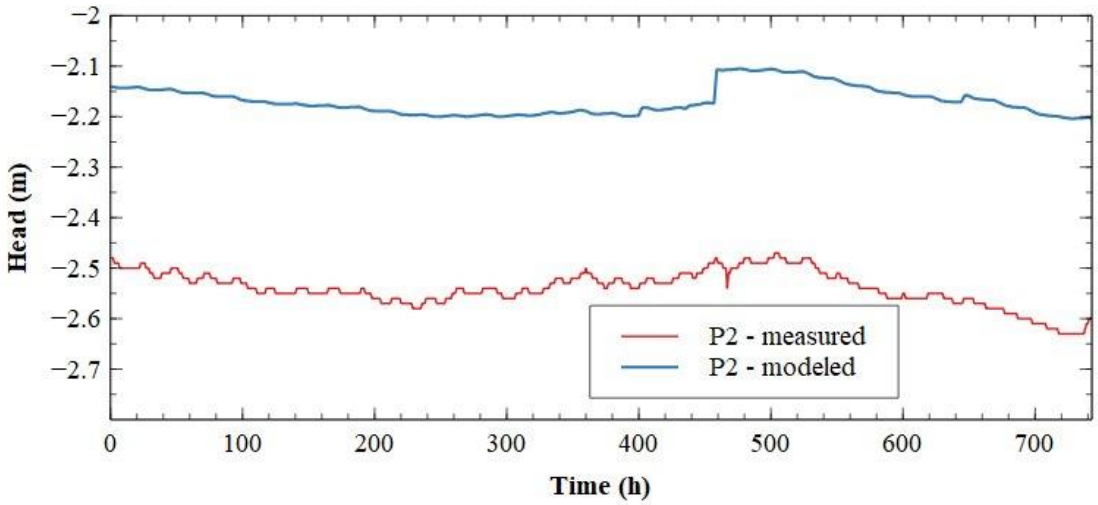

Figure 74 Measured and modelled head values for September 2021 on piezometer P2

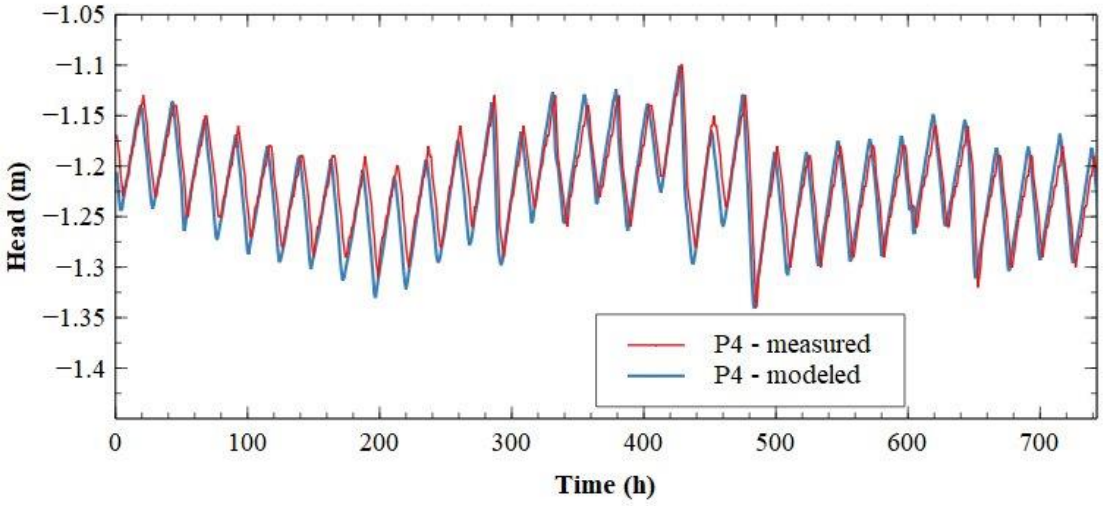

Figure 75 Measured and modelled head values for September 2021 on piezometer P4

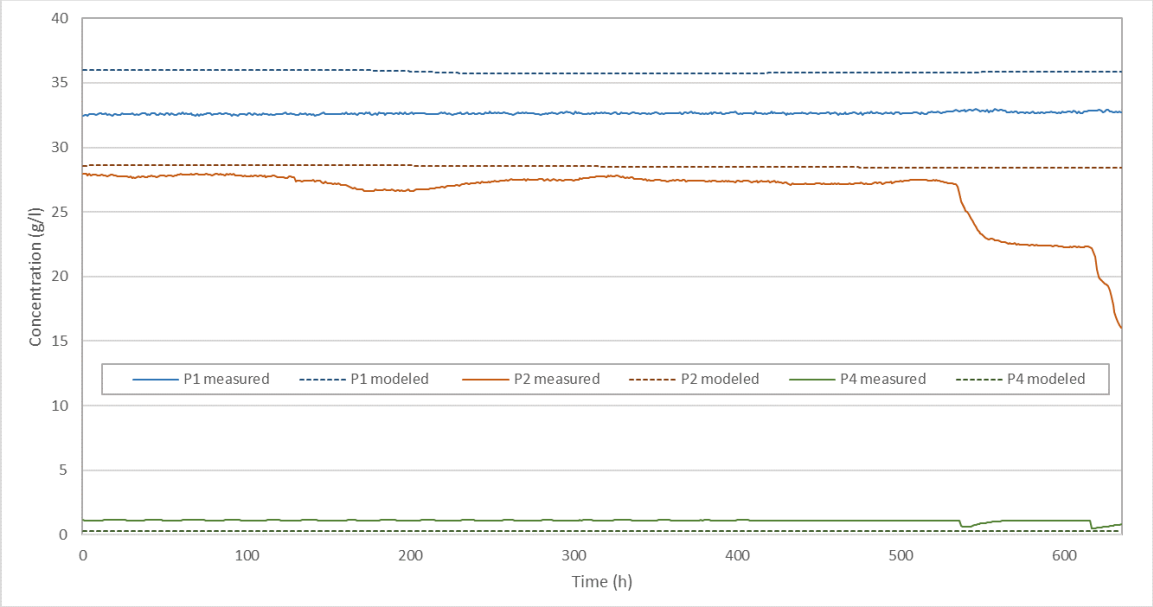

Figure 76 Measured and modelled concentration values for September 2021 on piezometers P1, P2 and P4

Conclusion

This report gives a comprehensive overview of model of existing state in the area of River Neretva Valley. Input parameters used as boundary conditions were measured values. Calibrated values (hydraulic conductivity, conductance of channels and specific flow) were based on data collected from the field. Besides the input parameters, report offers an overview of model scenarios and of process of calibration and verification.

Result section is divided in two groups for each step of modelling setup. First group offers results of head results and second offers salinity distribution for all piezometers. Calibration was carried out for head and concentration values in all piezometers.

After the process of calibration and verification was completed, it was possible to conclude that the model describes the existing state in the area of River Neretva Valley at a satisfactory level. Head modelled and measured values are in a quit a good match for all locations. Local deviation is due to external conditions. Measured concentration values are very stable during the time for all locations. Modelled concentration values are primarily based on steady state results and correspond to measured values. Based on obtained results it is possible to conclude that this model offers good foundation for further modelling of scenarios for climate changes and mitigation measures.

Bibliography

[1] Aquaveo, "GMS - Groundwater Modeling System." https://www.aquaveo.com/software/gms-groundwater-modeling-system-introduction

[2] M. G. McDonald and A. W. Harbaugh, "A modular three-dimensional finite-difference ground-water flow model," Tech. Water-Resources Investig., 1988.

[3] C. Zheng and P. Wang, "MT3DMS: A modular three-dimensional multispeces transport model for simulation of advection, dispersion, and chemical reactions of contaminants in groundwater systems.," US Army Corps of Engineers Engineer Research and Development Center, no. June. p. 239, 1998. [Online]. Available: http://www.geo.tu-freiberg.de/hydro/vorl_portal/gw-modellierung/MT3DMS Ref Manual.pdf

[4] C. D. Langevin, D. T. Thorne Jr., A. M. Dausman, M. C. Sukop, and W. Guo, "SEAWAT Version 4: A Computer Program for Simulation of Multi-Species Solute and Heat Transport," U.S. Geol. Surv. Tech. Methods B. 6, 2007.

[5] Aquaveo, "GMS User Manual (v10.3)." [Online]. Available: http://gmsdocs.aquaveo.com/GMS_User_Manual_v10.3.pdf

[6] C. E. Jacob, Flow of Groundwater in Engineering Hydraulic. New York: John Wiley & Sons, 1950.

[7] J. J. Jiao and Z. Tang, "An analytical solution of groundwater response to tidal fluctuation in a leaky confined aquifer," Water Resour. Res., vol. 35, no. 3, pp. 747–751, 1999, doi: 10.1029/1998WR900075.

[8] Y. Xia, H. Li, M. C. Boufadel, Q. Guo, and G. Li, "Tidal wave propagation in a coastal aquifer: Effects of leakages through its submarine outlet-capping and offshore roof," J. Hydrol., vol. 337, no. 3–4, pp. 249–257, 2007, doi: 10.1016/j.jhydrol.2007.01.036.

[9] Y. Ratner-Narovlansky, Y. Weinstein, and Y. Yechieli, "Tidal fluctuations in a multi-unit coastal aquifer," J. Hydrol., vol. 580, no. October, p. 124222, 2020, doi: 10.1016/j.jhydrol.2019.124222.

[10] H. Li and J. J. Jiao, "Tide-induced groundwater fluctuation in a coastal leaky confined aquifer system extending under the sea," Water Resour. Res., vol. 37, no. 5, pp. 1165–1171, 2001, doi: 10.1029/2000WR900296.

[11] M. Bakker, “The effect of loading efficiency on the groundwater response to water level changes in shallow lakes and streams,” Water Resour. Res., vol. 52, no. 3, pp. 1705–1715, 2016, doi: 10.1002/2015WR017977.

[12] V. Srzić, I. Lovrinović, I. Racetin, and F. Pletikosić, “Hydrogeological Characterization of Coastal Aquifer on the Basis of Observed Sea Level and Groundwater Level Fluctuations : Neretva Valley Aquifer , Croatia,” vol. 12, no. 2, p. 348, 2020, doi: 10.3390/w12020348.

List of figures

Figure 1 GMS modules 5
Figure 2 Spatial distribution of all boreholes in River Neretva Valley 11
Figure 3 Borehole log from 1960s 12
Figure 4 Borehole log from 2008 13
Figure 5 Resistivity sounding log 14
Figure 6 Resistivity sounding log transformed into borehole in GMS 14
Figure 7 Geoelectric tomography log 15
Figure 8 Geoelectric tomography log transformed in GMS cross-section 15
Figure 9 Geological characteristics of representative soil types 16
Figure 10 Bedrock surface in TIN Module 17
Figure 11 3D solid cross-sections 18
Figure 12 Conceptual model boundary and grid frame 20
Figure 13 3D Grid model 21
Figure 14 LPF Package dialog box 22
Figure 15 List of solver packages provided for MODFLOW in GMS 23
Figure 16 GMG Solver settings 24
Figure 17 List of MT3DMS packages provided in GMS 25
Figure 18 GCG solver setup 26
Figure 19 SEAWAT VDF Package 27
Figure 20 GMS optional packages 28
Figure 21 Boundary conditions defined with RIV package 30
Figure 22 Tide gauge and limnigraph values for July 2021 30
Figure 23 Conceptual model of the Neretva Valley aquifer 32
Figure 24 CHD boundary conditions for seawater and pumping stations 33
Figure 25 PS Prag and PS Modrič values for July 2021 34
Figure 26 Specified flow in the layer of gravel 35
Figure 27 Precipitation in period July-September 2021 36
Figure 28 Specified concentration boundary condition 37
Figure 29 Model steps 38
Figure 30 MODFLOW Global/Basic Package settings for flow steady state simulation 39
Figure 31 Concentration in one cell during the time and achievement of the steady state 40

Figure 32 Salinity field for winter period in surface layer 42
Figure 33 Salinity field for winter period in gravel layer 42
Figure 34 Cross-section of salinity field for winter period 43
Figure 35 Salinity field for summer period in surface layer 43
Figure 36 Salinity field for summer period in gravel layer 44
Figure 37 Cross-section of salinity field for summer period 44
Figure 38 Steady state head results for surface layer 45
Figure 39 Steady state head results for the layer of gravel 46
Figure 40 Head results in sand layer after 1 h for transient flow simulation 47
Figure 41 Head results in the layer of gravel after 1 h for transient flow simulation 47
Figure 42 Head results in the layer of gravel after 8 h for transient flow simulation 48
Figure 43 Head results in the layer of gravel after 16 h for transient flow simulation 48
Figure 44 Head results in the layer of gravel after 22 h for transient flow simulation 49
Figure 45 Head results for surface layer for flow and transport steady state simulation 51
Figure 46 Head results for gravel layer for flow and transport steady state simulation 51
Figure 47 Transport results for surface layer for flow and transport steady state simulation 52
Figure 48 Transport results for layer of gravel for flow and transport steady state simulation . 53
Figure 49 Measured and modelled head values for July 2021 on piezometer D1 55
Figure 50 Measured and modelled head values for July 2021 on piezometer D2 55
Figure 51 Measured and modelled head values for July 2021 on piezometer D3 56
Figure 52 Measured and modelled head values for July 2021 on piezometer D4 56
Figure 53 Measured and modelled head values for July 2021 on piezometer P1 57
Figure 54 Measured and modelled head values for July 2021 on piezometer P2 57
Figure 55 Measured and modelled head values for July 2021 on piezometer P4 58
Figure 56 Measured and modelled concentration values for July 2021 58
Figure 57 Adopted horizontal hydraulic conductivity values for the layer of sand 60
Figure 58 Adopted horizontal hydraulic conductivity values for the layer of gravel 61
Figure 59 Relation between specified flow, horizontal hydraulic conductivity and tidal efficacy for deep piezometers 62
Figure 60 Relation between specified flow, horizontal hydraulic conductivity and mean head value for deep piezometers 62
Figure 61 Measured and modelled head values for August 2021 on piezometer D1 63

Figure 62 Measured and modelled head values for August 2021 on piezometer D2 64
Figure 63 Measured and modelled head values for August 2021 on piezometer D3 64
Figure 64 Measured and modelled head values for August 2021 on piezometer D4 65
Figure 65 Measured and modelled head values for August 2021 on piezometer P1 65
Figure 66 Measured and modelled head values for August 2021 on piezometer P2 66
Figure 67 Measured and modelled head values for August 2021 on piezometer P4 66
Figure 68 Measured and modelled concentration values for August 2021 on piezometers P1, P2 and P4 67
Figure 69 Measured and modelled head values for September 2021 on piezometer D1 67
Figure 70 Measured and modelled head values for September 2021 on piezometer D2 68
Figure 71 Measured and modelled head values for September 2021 on piezometer D3 68
Figure 72 Measured and modelled head values for September 2021 on piezometer D4 69
Figure 73 Measured and modelled head values for September 2021 on piezometer P1 69
Figure 74 Measured and modelled head values for September 2021 on piezometer P2 70
Figure 75 Measured and modelled head values for September 2021 on piezometer P4 70
Figure 76 Measured and modelled concentration values for September 2021 on piezometers P1, P2 and P4 71